Distributed control and optimization for autonomous power grids

Dorfler, Florian; Bolognani, Saverio; Simpson-Porco, John W.; Grammatico, Sergio

DOI
10.23919/ECC.2019.8795974

Publication date
2019

Document Version
Accepted author manuscript

Published in
Proceedings of the 18th European Control Conference (ECC 2019)

Distributed Control and Optimization for Autonomous Power Grids

Florian Dörfler Saverio Bolognani John W. Simpson-Porco Sergio Grammatico

***Abstract*— The electric power system is currently undergoing a period of unprecedented changes. Environmental and sustainability concerns lead to replacement of a significant share of conventional fossil fuel-based power plants with renewable energy sources. As a result of this energy transition, centralized bulk generation based on fossil fuel and interfaced with synchronous machines is substituted by distributed generation based on renewables and interfaced with power electronic converters. Accordingly, the entire operation of power systems is undergoing several major paradigm shifts: from decentralized device-level control, over distributed coordination of energy sources, to real-time system-level optimization, and open markets involving demand response and energy storage.**

In this article, we give a tutorial introduction to new and emerging thrusts in analysis, control, and optimization of future, smart, and cyber-enabled power systems. The solutions that we present tap into some recent methodological advances in control and optimization, with a focus on the analysis of multi-agent decision scenarios and on the design of decentralized and networked control strategies. We cover the topics of decentralized control of power converters in low-inertia power systems, real-time control of distribution grids, optimal and distributed frequency control of transmission grids, and coordination of energy supply and demand. Throughout the article we also present worthwhile open directions for future research.

I. Introduction

Tomorrow's energy system and electric power grid are envisioned to be clean, sustainable, and largely based on renewable sources such as wind and solar power. As renewables are variable and interfaced through non-rotational generation, future power systems are subject to increasing fluctuations and uncertainties on all temporal and spatial scales. As a response to these challenges, more and more distributed resources such as micro-generators, storage, and flexible loads are being engaged in the demand and supply balancing process, energy markets are being opened up, and the stabilization of the electric power grid is shouldered on increasingly many decentralized actuators. Increased deployment of sensing, information, and communication technology provides the means to efficiently coordinate all of these devices. Hence, the power system is currently transitioning to a cyber-enabled system resulting in massive amounts of available data and unforeseen levels of sensing and actuation capabilities. Finally, electric mobility, energy-efficient homes, and consumer participation in general provide huge challenges as well as unprecedented opportunities to integrate an end-to-end automated and sustainable socio-technical system.

Parallel to these technological advances, the control, optimization, communication, computer science, and signal processing communities have developed novel methodological approaches addressing the challenges of future power systems: e.g., distributed optimization algorithms and efficient game-theoretic formulations have emerged to coordinate decentralized resources; decentralized and synchronization-based control methods have been developed for non-rotational generation; and some long-standing power system control, stability, and optimization problems have been resolved through methods from multi-agent and networked systems. There is no shortage of terms for such increasingly smart and end-to-end automated power systems, supplied by renewable energy, and enabled by networked-algorithms. We prefer the term "autonomous grids" coined in [1] which reflects decentralized and distributed system operation approaches – an angle that we also take in this article.

Power system control is nowadays a vibrant research area of the control community, and theory and practice enrich, nourish, and inspire one another. This article gives a tutorial introduction to the challenges of next-generation power systems and the energy transition from the perspective of systems control. We introduce the reader to several new and emerging thrusts in power system analysis, control and optimization. We also raise open questions that have yet to be addressed and present fruitful avenues for future research.

This article does not aim to be comprehensive in its scope, nor does it present all viewpoints and facets on the topics of power system control and optimization. Our exposition and treatment are colored by our own research interests and experiences. In particular, we focus here on the following topics: decentralized control of power converters in low-inertia power systems, real-time control of distribution grids, optimal and distributed frequency control of transmission grids, and coordination of energy supply and demand. There is a broad range of challenging control and optimization problems in future power system that are not (or only tangentially) discussed in this article including the following: wide-area control – a continental-scale distributed control for power system oscillation damping – is discussed in the recent surveys [2]–[4]; novel algorithmic and distributed approaches to optimal power flow (OPF) methods are discussed in the reviews [4]–[7]; DC technologies become ever more prevalent in HVDC grids [8]–[10] and in DC microgrids [11]–[13]; and finally there is a rich emerging literature on distributed and hierarchical control in microgrids [14]–[16].

This work was supported in part by ETH Zürich Funds, SNF AP Energy Grant #160573, SFOE grant #SI/501708 UNICORN, NSERC DG RGPIN-2017-04008, NWO (OMEGA, 613.001.702; P2P-TALES, 647.003.003), and the ERC (COSMOS, 802348).

F. Dörfler and S. Bolognani are with the Automatic Control Laboratory at ETH Zürich, Switzerland email: [dorfler,bsaverio]@ethz.ch. J. W. Simpson-Porco is with the University of Waterloo, Canada, email: jwsimpson@uwaterloo.ca. Sergio Grammatico is with TU Delft, The Netherlands, email: s.grammatico@tudelft.nl.

The remainder of this article is organized as follows. Section II focuses on decentralized power converter control. Section III covers real-time distribution grid control. Section IV discusses distributed frequency control. Section V addresses supply and demand coordination. Finally, Section VI concludes the paper and presents open research directions.

II. Decentralized Control of Power Converters in Low-Inertia Power Systems

At the heart of the energy transition is the change in generation technology: from conventional rotational power generation based on synchronous machines (SM) towards power converter-interfaced generation (CIG), as in the case of renewable energy sources, battery storage, or high-voltage DC (HVDC) links interconnecting different synchronous areas. This transition poses major challenges to the operation, control, and stability of the power system due to

(i) the loss of rotational kinetic energy in the SM whose inertia acts a safeguard against disturbances;
(ii) the loss of the stable and robust nonlinear synchronization mechanism which is physically inherent to SMs;
(iii) the loss of the robust frequency and voltage control (since SMs are the main points of actuation); and thus
(iv) the loss a stable global frequency signal altogether (which is the basis for many services; see Section IV).

In future low-inertia power systems, all of these functionalities have to be provided by control of power converters, which – in absence of *control* – lack all of the above features. These so-called *low-inertia* challenges are currently regarded as one of the ultimate bottlenecks to massively integrating renewables in power systems around the world.

We refer to [17]–[23] surveying the challenges of low-inertia systems and possible solution approaches. In what follows, we give a tutorial introduction from the perspective of control theory, present the models of SMs and CIGs, their control specifications, and different control approaches.

A. Models of Synchronous Machines and Power Converters

We refer to [24]–[27] for control-theoretic expositions and the text books [28]–[33] concerning the modeling of circuits, voltage source converters (VSCs), and SMs. We consider a three-phase AC power system, and assume that all phases are balanced and all impedances are symmetric. This allows us to express all AC quantities as two-dimensional variables, e.g., in rectangular $\alpha\beta$-coordinates, rotating (with a reference frequency) dq-coordinates, polar (complex-valued) phasor coordinates, or combinations thereof. For simplicity, we choose $\alpha\beta$-coordinates in what follows. While there are many SM and VSC models, we consider two prototypical models shown in Figures 1-2 used among others in [34], [35].

SM model The SM converts mechanical to electrical energy via a rotational magnetic field with inductance matrix

$$L_\theta = \begin{bmatrix} L_\mathrm{s} & 0 & L_\mathrm{m}\cos\theta \\ 0 & L_\mathrm{s} & L_\mathrm{m}\sin\theta \\ L_\mathrm{m}\cos\theta & L_\mathrm{m}\sin\theta & L_\mathrm{r} \end{bmatrix}$$

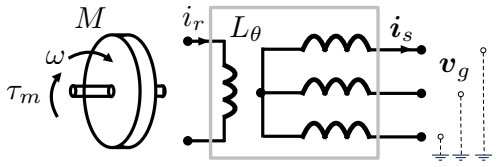

Fig. 1. Sketch of a simple (permanent magnet) synchronous machine (SM)

coupling the currents $\boldsymbol{i}_s \in \mathbb{R}^2$ and $i_r \in \mathbb{R}$ of the SM stator and rotor, respectively. The electromagnetic field is driven by the generator rotor with angle $\theta \in \mathbb{S}^1$ and frequency $\omega \in \mathbb{R}$. The mechanical rotor swing and stator flux dynamics are

$$\frac{\mathrm{d}\theta}{\mathrm{d}t} = \omega \tag{1a}$$

$$M\frac{\mathrm{d}\omega}{\mathrm{d}t} = -D\omega + \tau_m + L_\mathrm{m} i_r \left[\begin{smallmatrix} -\sin\theta \\ \cos\theta \end{smallmatrix}\right]^\top \boldsymbol{i}_s \tag{1b}$$

$$L_\mathrm{s}\frac{\mathrm{d}\boldsymbol{i}_s}{\mathrm{d}t} = -R_s\boldsymbol{i}_s + \boldsymbol{v}_g - L_\mathrm{m} i_r \left[\begin{smallmatrix} -\sin\theta \\ \cos\theta \end{smallmatrix}\right]\omega\,, \tag{1c}$$

where all parameters are as depicted in Figure 1, $\boldsymbol{v}_g \in \mathbb{R}^2$ is the AC (grid) voltage at the SM terminals, D and R_s model the mechanical and electrical dissipation, τ_m is the mechanical control input (relatively slow actuation typically used for speed droop and automatic generation control (AGC)), and i_r is the excitation rotor current control input (fast actuation used for automatic voltage regulation (AVR) and damping control). More detailed higher-order models consider additionally the mechanical (turbine governor) actuation stage, the rotor flux dynamics, and stabilizing damper windings.

VSC model The VSC converts a DC voltage $v_\mathrm{dc} \in \mathbb{R}$ and current $i_x \in \mathbb{R}$ to an AC voltage $v_x \in \mathbb{R}^2$ and inductor current $\boldsymbol{i}_f \in \mathbb{R}^2$ by modulating the converter switches as

$$i_x = -\boldsymbol{m}_{\alpha\beta}^\top \boldsymbol{i}_f \quad \text{and} \quad \boldsymbol{v}_x = \boldsymbol{m}_{\alpha\beta}^\top v_\mathrm{dc}\,,$$

where $\boldsymbol{m}_{\alpha\beta} \in [-1/2, 1/2] \times [-1/2, 1/2]$ are the normalized duty cycle ratios. Here we consider an averaged model where $\boldsymbol{m}_{\alpha\beta}$ is a continuous variable, typically parameterized as

$$\boldsymbol{m}_{\alpha\beta} = u_\mathrm{mag} \left[\begin{smallmatrix} -\sin\delta \\ \cos\delta \end{smallmatrix}\right] \quad \text{and} \quad \dot{\delta} = u_\mathrm{freq}\,,$$

where $u_\mathrm{freq} \in \mathbb{R}$ and $u_\mathrm{mag} \in [-1/2, 1/2]$ are the controllable switching frequency and magnitude. The overall VSC is then

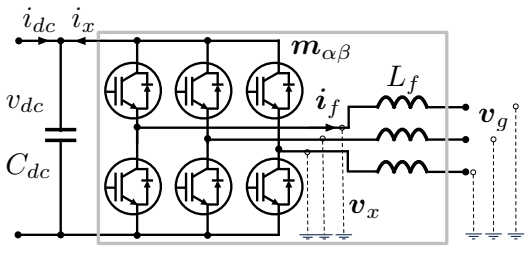

Fig. 2. Sketch of a two-level voltage source converter (VSC)

modeled by the DC capacitor and AC inductor dynamics

$$\frac{\mathrm{d}\delta}{\mathrm{d}t} = u_{\text{freq}} \tag{2a}$$

$$C_{\text{dc}}\frac{\mathrm{d}v_{\text{dc}}}{\mathrm{d}t} = -G_{dc}v_{\text{dc}} + i_{\text{dc}} + u_{\text{mag}}\left[\begin{smallmatrix}-\sin\delta\\ \cos\delta\end{smallmatrix}\right]^{\top}\boldsymbol{i}_f \tag{2b}$$

$$L_f\frac{\mathrm{d}\boldsymbol{i}_f}{\mathrm{d}t} = -R_f\boldsymbol{i}_f + \boldsymbol{v}_g - u_{\text{mag}}\left[\begin{smallmatrix}-\sin\delta\\ \cos\delta\end{smallmatrix}\right]v_{\text{dc}}\,, \tag{2c}$$

where all parameters are as in Figure 2, G_{dc} and R_f model the lumped switching and conduction losses, $\boldsymbol{v}_g \in \mathbb{R}^2$ is the AC voltage at the VSC terminals, and i_{dc} is the controllable DC-side current typically coming from an upstream DC converter or storage element. Aside from an upstream converter, higher-order CIG models consider additionally LC or LCL filters at the AC terminals rather than a single inductor.

B. Similarities, Differences, and Control Limitations

The SM and VSC models (1) and (2) can be abstracted as a power-preserving interconnection of energy supply, conversion, and storage [36]: from a controllable supply (via τ_m and i_{dc}), over storage (via M and C_{dc}), a nearly lossless conversion (or signal transformation) (via L_θ and $\boldsymbol{m}_{\alpha\beta}$) that is controllable (via i_r and $\boldsymbol{m}_{\alpha\beta}$), to the AC grid; see Figure 3.

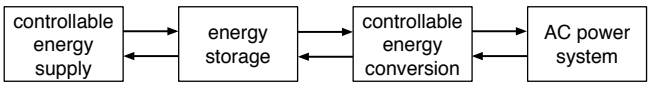

Fig. 3. Conceptual abstraction of VSC and SM control systems

Structural similarities On a less abstract level, note the similarity of the SM and VSC models: when controlling the VSC frequency proportional to its DC voltage, e.g., as

$$u_{\text{freq}} = \eta v_{\text{dc}}\,, \tag{3}$$

where $\eta = \omega_{\text{ref}}/v_{\text{dc,ref}}$ is chosen as the ratio of the nominal AC grid frequency ω_{ref} and DC voltage $v_{\text{dc,ref}}$, then the SM model (1) and closed-loop VSC (2)-(3) are *structurally equivalent* when identifying $\theta \equiv \delta$, $\omega \equiv \eta v_{\text{dc}}$, $\boldsymbol{i}_s = \boldsymbol{i}_f$, and $u_{\text{mag}} = L_m i_r$. Accordingly, we can match the associated parameters, e.g., the equivalent inertia M as the normalized DC capacitance C_{dc}/η^2 and the imbalance (kinetic energy) signal ω as v_{dc}. These analogies and electro-mechanical dualities have recently given rise to a variety of control methods primarily based on the DC voltage as control signal and DC capacitor as equivalent inertia [17], [34], [37]–[40]. We will return to these control strategies in Section II-D.

Deceiving similarities The above similarities can be misleading, as highlighted in the following key observation. The power balance of the SM (neglecting the comparatively small magnetic energy and dissipation) amounts to [26], [35]

$$\underbrace{\tfrac{d}{dt}\omega^{\top}M\omega}_{\text{change kinetic energy}} = \underbrace{\omega^{\top}\tau_m}_{\text{mechanical power supply}} - \underbrace{\boldsymbol{i}_s^{\top}\boldsymbol{v}_g}_{\text{power demanded by grid}}\,. \tag{4}$$

Thus, any power imbalance (e.g., caused by a grid fault) will be absorbed in the SM's kinetic energy before any restoring control mechanism via τ_m even acts. The power

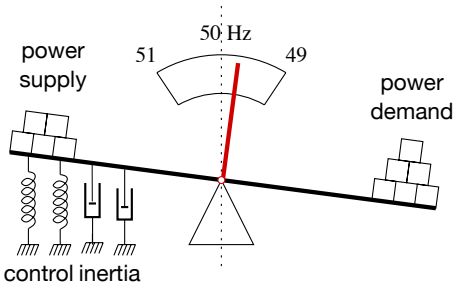

Fig. 4. Mechanical analogue of the power balance (4) adapted from [41]

balance equation (4) is illustrated in Figure 4 via a simplified mechanical analogue, where we also indicated control mechanisms (discussed in Section II-C). While under similar assumptions an analogous power balance holds for the VSC,

$$\tfrac{d}{dt}v_{\text{dc}}^{\top}C_{\text{dc}}v_{\text{dc}} = v_{\text{dc}}^{\top}i_{\text{dc}} - \boldsymbol{i}_f^{\top}\boldsymbol{v}_g\,,$$

the equivalent inertia in the DC capacitor is rather small and its effect as a safeguard against disturbances is negligible. However, as an opportunity, the equivalent actuation and energy supply i_{dc} is rather fast compared to τ_m.

Control limitations The above insights lead to the following characteristics of SMs and VSCs as control systems:

- fast vs. slow actuation of the energy supply: the turbine-governor input τ_m of a SM is rather slow, whereas the VSC DC input i_{dc} can be controlled very fast (though i_{dc} is typically constrained in power and energy);
- significant vs. negligible energy storage: since M is orders of magnitudes larger than C_{dc}, SMs are much more robust to disturbances than VSCs (c.f., low-inertia);
- limited vs. full AC actuation: the SM's excitation control via the single input i_r is complex (and often limited in practice), whereas the VSC's AC voltage $\boldsymbol{v}_x = \boldsymbol{m}_{\alpha\beta}^{\top}v_{\text{dc}}$ is fully controllable (unless $v_{\text{dc}} = 0$) through the two modulation inputs u_{freq} and u_{mag}; and
- state constraints: whereas an SM can tolerate large fault currents (up to a factor 6–10 above nominal), the VSC's switches cannot withstand any over-currents.

In summary, SMs and VSCs share lots of structural similarities, but they have nearly antipodal control characteristics.

C. Control Specifications and Classic Control Approaches

We specify the control objectives separately as nominal steady-state, perturbed steady-state, and transient objectives since the conventional power system stability classification and associated controllers also make such distinctions [30]. We additionally discuss slower time-scale objectives such as secondary regulation and tertiary set-point (re)scheduling that will be addressed in the forthcoming sections.

Nominal steady-state specifications During nominal system operation at frequency ω_{ref}, the requirements on a *synchronous steady state* are as follows [42], [43]:

(S1) all DC states need to be constant, that is, $\dot{\omega} = \dot{v}_{\text{dc}} = 0$;
(S2) all AC states need to be synchronous at ω_0, that is, $\dot{\theta} = \dot{\delta} = \omega_{\text{ref}}$, $\frac{\mathrm{d}}{\mathrm{d}t}\boldsymbol{i}_s = \left[\begin{smallmatrix}0 & \omega_{\text{ref}}\\ -\omega_{\text{ref}} & 0\end{smallmatrix}\right]\boldsymbol{i}_s$, and so on; and

(S3) for the VSC (and analogously for the SM) the active power $P \triangleq \boldsymbol{i}_s^\top \boldsymbol{v}_g$, reactive power $Q \triangleq \boldsymbol{i}_s^\top \left[\begin{smallmatrix} 0 & -1 \\ 1 & 0 \end{smallmatrix}\right] \boldsymbol{v}_g$, and terminal voltage magnitude $\|\boldsymbol{v}_g\|$ take pre-specified values P_{ref} and Q_{ref} and $\boldsymbol{v}_{\text{ref}}$, respectively.

These set-points are scheduled offline; see specification (S6).

Perturbed steady-state specifications The power system typically fluctuates around a nominal stationary operating point due to variable generation, loads, and disturbances. Aside from high-frequency perturbations, the system typically operates at a synchronous frequency ω_0 different from ω_{ref}, i.e., all signals satisfy the specifications (S1) and (S2) above with ω_{ref} replaced by ω_0. Additionally, grid codes (grid interaction protocols) demand pre-specified sensitivities, so-called *droop slopes* $\partial P/\partial\omega$ (resp., $\partial Q/\partial\|\boldsymbol{v}_g\|$) prescribing a linear trade-off between power injection, frequency, and voltage [28]–[30]. For example, (S3) changes to

(S4) *droop specification:* $P = P_{\text{ref}} - K \cdot (\omega - \omega_{\text{ref}})$,

where $K > 0$ is the droop slope. Similar droop specifications exist for Q and $\|\boldsymbol{v}_g\|$ [44], [45], and they are typically enforced via proportional (also called *primary* or *droop*) control of the VSC inputs i_{dc} (or also u_{freq}) or the SM input τ_m (resp., the modulation amplitude u_{mag} or excitation current i_r) as function of the frequency deviation (resp., the voltage deviation), see [28], [29] and also Sections III-IV.

Since droop control provides physical energy to the system and results in generation costs, the actual values of the droop slopes $\partial P/\partial\omega$ (resp., $\partial Q/\partial\|\boldsymbol{v}_g\|$) are negotiated in ancillary service markets (see Section V) or determined by grid codes, e.g., inversely proportional to the generation capacity.

Regulation specification In a perturbed steady state, the synchronous frequency ω_0 is a *global signal* that reflects the load/generation imbalance, which can be seen by evaluating the power balance (4) for a constant $\omega(t) = \omega_0$. The non-trivial insight is that the global system imbalance can be inferred locally by measuring ω; see also Figure 4 for an illustration. Hence, the synchronous frequency is used as a *floating variable* that indicates imbalance, serves as a control signal, and is regulated only longer time scales (on the order of minutes) by means of *secondary* (integral) control approaches (see Sections III-IV for details):

(S5) *secondary regulation:* regulate ω_0 to ω_{ref}.

Similar arguments apply to voltage magnitudes, though they do not carry global information and are regulated tighter.

Set-point specifications The pre-specified power and voltage set-points for the nominal steady state are computed offline, e.g., through an OPF or via various markets; see Sections III-IV for details. This set-point scheduling must be consistent (i.e., the physical power balance equations must be feasible), satisfy operational constraints (e.g., voltage limits), and typically minimize an economic dispatch criterion [46]:

(S6) the set-points P_{ref}, Q_{ref}, and $\boldsymbol{v}_{\text{ref}}$ need to be consistent, satisfy operational limits, and be economically efficient.

Often these set-points have to be updated during operation time and generators have to be re-dispatched. This set-point (re)scheduling is typically referred to as *tertiary control*.

Transient specifications Finally, the grid should be robust to perturbations. Especially, on the fast, so-called *transient*, time scale (up to five seconds), where

(S7) transient disturbances and faults need to be rejected.

For SMs disturbance rejection is achieved passively via their large inertia M and actively via Power System Stabilizers (PSSs) inducing damping by closing a control loop between ω and i_r [28]. This classic SM control problem has been approached from many angles [47]–[49]. However, the rejection of large disturbances is still an unresolved and contested problem for CIGs, which is at the heart of making low-inertia systems reliable. In the next section, we will give an introduction and overview of the proposed control solutions.

We conclude this section with Figure 5 which summarizes the different control actions that need to be undertaken to meet the specifications (S1)–(S7). The next subsection will focus on the fastest time scale and the control of CIG. Sections III, IV, and V will address the slower secondary and tertiary time scales – though noting that these nominally slower control actions get ever closer to real-time operation.

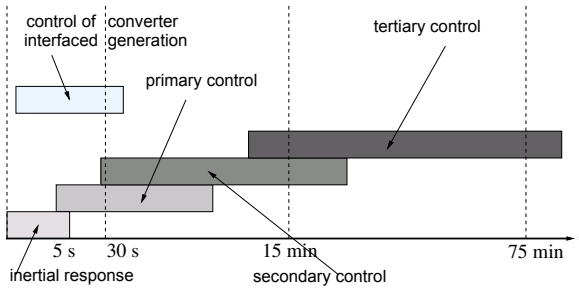

Fig. 5. Time scales of power system control operation adapted from [18]

D. Decentralized Control of Power Converters

Forming and following classifications Since power converters are fast, modular, and nearly fully actuated control systems, a vast number of articles discuss different control architectures and tuning criteria. For the considered grid-connected converters, an important classification is that of *grid-following* and *grid-forming* control [18]. While there is no universally accepted definition of these concepts (whose exact distinctions are often vigorously debated), we provide in the following a control-theoretic characterization in terms of system behavior [50], causality, and reachability:

1) steady-state behavior: grid-following converters measure the grid frequency (e.g., by passing $\boldsymbol{v}_g$ to a phase-locked loop (PLL)), command their modulation frequency u_{freq} to track this measured frequency, and regulate their terminal current to meet a specification, e.g., a (P, Q) set-point or a droop. For these reasons, grid-following converters are referred to as "frequency-following" and "current-controlled".

In comparison, grid-forming converters are "frequency-forming", "voltage-controlled"[1], and invert inputs and out-

[1]A voltage-controlled converter is interfaced to the grid through an LC filter, that is, an AC-side capacitor is added to the VSC in Figure 2.

puts: the terminal voltage frequency and magnitude are controlled, e.g., based on active power measurement as in droop

$$u_{\text{freq}} = \omega_{\text{ref}} - \tfrac{1}{K} \cdot (P - P_{\text{ref}}) \,, \tag{5}$$

with droop slope $K > 0$, or as in the matching control (3).

2) reachability: grid-following converters require a strong grid with stiff frequency, which they can track. In absence of a grid, they lack their driving input and will not output a sinusoidal wave-form. In comparison, grid-forming converters can *reach* the desired behavior, i.e., "form the grid frequency and voltage", and can thus function in islanded mode (e.g., when connected only to a resistor). By this classification, a constant feedforward modulation, e.g., $u_{\text{freq}} = \omega_{\text{ref}}$ and $u_{\text{mag}} = 1$ p.u., is forming a grid, but it cannot adapt to ambient conditions (such as a shortage or surplus of generation), cannot produce a floating frequency (indicating the global imbalance), and finally such a feedforward scheme is not robust to clock drifts [51], [52]. For this reason, grid-forming converters are controlled in feedback, e.g., by droop (5).

Other desirable features of droop control are that it induces a frequency consensus (thus grid-forming converters can synchronize with another or with a stiff grid), and it achieves fair power sharing, that is, any load/generation imbalance is picked up equally according to the droop slopes [53]–[55].

Limitations of grid-following control Simplified models of grid-following and grid-forming converters give rise to the same input/output behavior (e.g., a droop specification), but their controllers have different inputs and outputs (which can make a significant difference, e.g., when measuring a brittle frequency), different performance characteristics (e.g., grid-following converters are limited by the accuracy and the bandwidth of their PLLs), and they can function with either only strong or also with weak grids. Thus far, grid-following converters were dominating in conventional grids where CIG was not required to provide any ancillary control services – other than injecting free renewable energy. However, future low-inertia power systems require grid-forming converters that take over the role of SMs, form the frequency and voltage, reject disturbances, and provide ancillary services, such as frequency droop, reactive power support, and fast (inertial) frequency response to stabilize the grid.

Overview of grid-forming strategies There are manifold proposals how to control grid-forming converters; see the reviews and comparison studies [17], [18], [56]–[59]. The bulk of which can be classified into four distinct groups that all have to cope with the limitations reviewed in Section II-B.

The first and most developed approach is **droop control** as in (5) and regulation of the terminal voltage $\|\boldsymbol{v}_g\|$ through u_{mag}. While droop control is well-studied and understood, stability characterizations exist only for simplified models [53]–[55] and practical implementation usually demands various extra heuristics such as low-pass filters or virtual impedances inducing damping in the control loop. Finally, droop control closes two independent SISO loops separately for P and ω as well as for Q and $\|\boldsymbol{v}_g\|$. However, these quantities are actually coupled especially when far away from a nominal steady state which leads to a poor transient performance of droop and a limited basin of attraction.

A second approach is based on emulation of **virtual SMs** making sure that the terminal behavior of the VSC (2) equals that of a SM (1); see e.g. [17], [32], [56], [59]. The core of this approach is a reference system, e.g., a software model of the SM (1) on a micro-controller, driven by measurements of the terminal signals $(\boldsymbol{i}_f, \boldsymbol{v}_g)$, and the output of which serves as reference signal for controlling the modulation $(u_{\text{freq}}, u_{\text{mag}})$ typically via (cascaded) PI tracking controllers. The appeal of the virtual SM approach is backward compatibility to the legacy system, but it suffers from various practical drawbacks such as time delays in control loopst, overshoots, and current violations. Since SMs and VSCs have antipodal characteristics (as argued Section II-B), it seems shortsighted to control a VSC (without storage though fast) to mimic a SM (with large storage and slow actuation) [18].

A third approach is **virtual oscillator control** (VOC) [60]–[64] which uses a nonlinear oscillator as reference system reminiscent of the classic van der Pol model. Based on recent theoretic developments in the synchronization of coupled oscillator models, it can be shown that such oscillator-controlled inverters robustly and almost globally synchronize [60], [61], even when pre-specified set-points are assigned [63], [64], and it locally (near steady-state) reduces to droop control [62]. Thus, VOC is a global and multivariable (taking cross-coupling into account) implementation of droop control which generally appears to be faster and more robust [58].

Fourth and finally, the **matching control** approaches [34], [37]–[40] reviewed in Section II-B rely on the VSC and SM dualities and match the SM's power conversion mechanism (the rotating electro-magnetic field) by the control (3). A notable feature compared to all other approaches is that the converter AC control makes use of a DC signal, whereas the previous three approaches decouple AC and DC sides, and stabilize the latter through SISO P(I)-controls. Thus, unsurprisingly due to its multivariable nature, there are scenarios when the matching control (3) is resilient to a disturbance whereas the other three controllers fail [57].

We close here by stating that quest for the "best" grid-forming control is still vigorously debated accross communities, and the field is enjoying tremendous interest right now. Finally, all the presented device-level controllers can give excellent system-level performance when their gains tuned well [65], and their set-points are regularly updated (which will be one of the subjects of the forthcoming sections).

III. Real-Time Control of Distribution Grids

A. Challenges in Future Power Distribution Grids

One of the consequences of the integration of renewable energy sources in the generation mix is the additional stress faced by power distribution grids. In fact, most renewable sources are interfaced to the grid through power converters and are deployed as small scale installations (microgenerators) in the low and medium voltage power network, rather than in the high voltage transmission grid. Power distribution lines have non-neglibile resistance and their power transfer

capacity is limited. Because of these reasons, congestion phenomena are expected to occur increasingly often: voltage collapse/instability, violation of voltage limits, and line and transformer overloading [66].

In order to guarantee a safe, reliable, and efficient operation of these grids, microgenerators must be provided with appropriate set-points, as already discussed in Section II-C (specification S6). In transmission grids, generator set-points are typically scheduled via offline programming, by solving an Optimal Power Flow problem in which economic cost is minimized based on relatively accurate models of the grid and of the power demand profiles. The same approach is generally unfeasible for distribution grids: the power demand of each distribution bus is often unmonitored and highly uncertain, and network parameters are often known with significant error. Moreover, the flexibility and the fast dynamic response of microgenerators allow to update set-points at a much faster rate than the traditional time scale of tertiary control depicted in Figure 5. This increased responsiveness is expected to be critical for the efficient accomodation of fluctuating and intermittent renewable sources.

In this section, we will therefore present a recent research trend, consisting in the design of *responsive* and *automated* strategies to update the generator set-points in real-time, based on measurements collected from the grid (either by the same microgenerators or by dedicated sensors). As represented schematically in Figure 6, this approach can be interpreted as a *feedback* approach to set-point generation, in contrast to the *feedforward* nature of optimization-based schemes. The two main advantages of a feedback architecture are its robustness to model mismatch and its capability to reject exogenous disturbances without measuring them (in this application, disturbances represent for example unmonitored load demands). Both these points will be elaborated in the rest of this section. Another important advantage of a feedback optimization approach is the availability of rigorous methods to design the controller so that the dynamic performance of the closed-loop system is improved (i.e., time-varying disturbances are tracked while ensuring that the interconnection with the system dynamics does not introduce instabilities).

Instead of reviewing the relevant pieces of work from the literature here, we will first present a unified formulation of this feedback strategy and we will then discuss the main design challenges one at a time, referring the reader to different solutions available in the recent literature.

We will not cover the dynamic part of the control design in this section, which is a thriving topic on its own. We can refer the reader to some very recent works on this matter [67]–[73].

Finally, it is important to notice that while distribution grids constitute a very compelling motivation and benchmark for this strategy, most of the proposed methods can be applied to transmission grids as well. In fact, some of the contributions that we will review have a broader scope than the distribution systems.

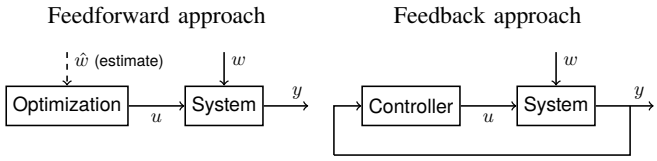

Fig. 6. A schematic illustration of the difference between the standard optimization approach to the generation of set-points and the proposed feedback solution. The signal u, y, and w, denote decision variables, measurements, and exogenous parameters of the optimization problem, respectively.

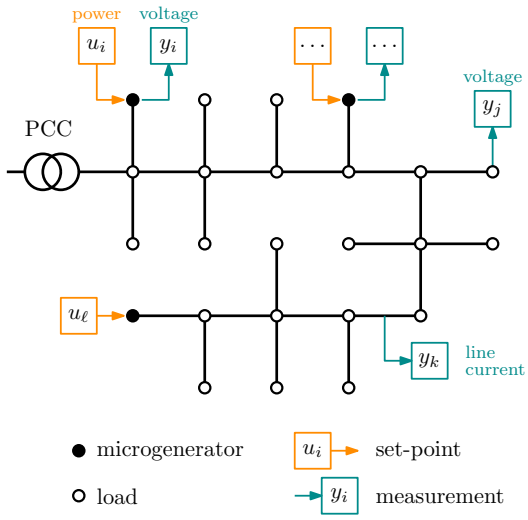

Fig. 7. An example of the control architecture that we assume in a power distribution grid, highlighting the available measurements and the controlled variables (set-points).

B. Distribution Grid Modeling and Control Architecture

We consider the control architecture that is schematically represented in Figure 7. The diagram represent a power distribution grid that hosts multiple loads and microgenerators. We denote

- by u the vector of *set-points* for the microgenerators; as explained in Section II, these can be set-points for the active and reactive power injection, or for the voltage magnitude;
- by y the vector of *measurements* that we perform on the grid; these outputs can include for example voltage magnitudes, line currents, and power flows.

When the grid is at steady state (including electrical transients, load dynamics, and the local controllers reviewed in Section II), the output y converges to a steady-state value

$$y^* = h(u, w), \tag{6}$$

that is function both of the set-points u and of a vector w of exogenous inputs (e.g., power demand of the loads at all buses, substation voltage).

The steady-state map h descends directly from Kirchhoff laws from the tracking characteristics of local controllers. It will become clear later that an explicit knowledge of h is not needed for the control design procedure presented in this section. It is however necessary to guarantee its existence

and well-posedness. To illustrate this point with an example, consider a distribution grid in which v, θ, p and q denote the bus voltages, angles, active power injection, and reactive power injection, respectively. We can partition these vectors as

$$v = \begin{bmatrix} v_0 \\ v_G \\ v_L \end{bmatrix}, \quad \theta = \begin{bmatrix} \theta_0 \\ \theta_G \\ \theta_L \end{bmatrix}, \quad p = \begin{bmatrix} p_0 \\ p_G \\ p_L \end{bmatrix}, \quad q = \begin{bmatrix} q_0 \\ q_G \\ q_L \end{bmatrix},$$

where the first element of each vector refers to the substation, the subvectors with subscript G refer to the buses that host a microgenerator (and no loads), while the remaining subvectors with subscript L refer to load buses. By Kirchhoff laws, the electrical state of the grid needs to satisfy at steady state

$$\mathrm{diag}(\nu)\overline{Y\nu} = p + jq, \tag{7}$$

where ν denotes the vector of complex bus voltages $\nu_i = v_i e^{j\theta_i}$, and where Y is the bus admittance matrix. Equation (7) can be interpreted as an implicit relation between the quantities that we introduced before:

$$f(v, \theta, p, q) = 0. \tag{8}$$

Let us assume that we can control the power set-points for the generator buses with no tracking error ($u = \left[\begin{smallmatrix} p_G \\ q_G \end{smallmatrix}\right]$) and we can measure their voltage ($y = v_G$), while all other power demands and the substation voltage are uncontrolled ($w = [v_0 \ \theta_0 \ p_L^\top \ q_L^\top]^\top$). The vectors u, y, and w are therefore a simple rearrangement of the coordinates v, θ, p, q. The existence of an explicit nonlinear function $y = h(u, w)$ that solves (8) can be guaranteed, for example, in the neighborhood of the no-load solution [74], [75], although a closed-form expression is, in general, not available.

C. Real-Time Control Specifications

We now elaborate the set-point specifications that have been introduced as (S6) in Section II. Set-points for the generators need to be compatible with the power flow equations and with the power demand on the system, they need to satisfy some operational limits of the grid, and they need to be economically efficient. We unify these specifications via the following general non-convex Optimal Power Flow program:

$$\begin{aligned} \min_{u,y} \quad & J(u, y) && \text{(9a)} \\ \text{subject to} \quad & g(y) \leq 0 && \text{(9b)} \\ & u \in \mathcal{U} && \text{(9c)} \\ & y = h(u, w), && \text{(9d)} \end{aligned}$$

where $g(y) \leq 0$ describes operational constraints of the grid (e.g., voltage limits) and $\mathcal{U}$ is the set of feasible set-points which we assume to be compact.

In the example introduced before, where $u = \left[\begin{smallmatrix} p_G \\ q_G \end{smallmatrix}\right]$ and $y = v_G$, the set $\mathcal{U}$ would describe the power capability limits of microgenerators, while $g(y)$ could be used to describe under- and over-voltage bounds: $g(y) = \left[\begin{smallmatrix} v_G - v_G^{\max} \\ v_G^{\min} - v_G \end{smallmatrix}\right] \leq 0$.

In the following, we assume that the constraint (9b) is replaced by an opportune penalty function, yielding the following optimization program

$$\min_{u \in \mathcal{U}} \ \underbrace{J(u, h(u, w)) + \psi(h(u, w))}_{=:\phi(u)} \tag{10}$$

where $\psi(y)$ is a scalar-valued transformation of $g(y)$.

Note that the optimization program (10) cannot be solved offline, because the exogenous input w (which we assume constant for the time scale of interest) is unknown. This prevents the application of optimal power flow solvers (even distributed one, e.g. [76], [77]) for this task. Strictly speaking, the feedback optimization methods proposed in [78] would also be unsuited for this task, as they assume full grid state measurement (although the underlying methodology is similar to the one presented in this section). Moreover, uncertainty in the grid parameters translates into uncertainty on the nonlinear map h, and consequently on the evaluation of the penalty function for the constraint (9b).

In the rest of this section, we will consider a specific line of attack to this challenge, inspired by gradient-descent methods for nonlinear optimization. It is not however the only possible strategy: we will review a few other options at the end of the section. Nevertheless, the formulation that we present hereafter is sufficient to highlight the key features and, more importantly, the main challenges that characterize this control design problem.

D. Gradient Flow Design

We consider the key problem of designing a continuous-time gradient descent flow that converges to the (local) minimizer of (10). Note that the gradient $\nabla\phi(u)$ can be computed explicitly as

$$\begin{aligned} \nabla\phi(u) = \ & \nabla_u J(u, h(u, w)) + \\ & \nabla_u h(u, w)^\top \nabla_y J(u, h(u, w)) + \\ & \nabla_u h(u, w)^\top \nabla \psi(h(u, w)). \end{aligned} \tag{11}$$

Once $\nabla\phi(u)$ is available, (10) can be tackled via standard iterative solvers, e.g., to drive a projected gradient descent method of the form

$$\dot{u} \in \Pi_{T_u\mathcal{U}}\left[-\nabla\phi(u)\right] := \arg\min_{v \in T_u\mathcal{U}} \|v - (-\nabla\phi(u))\|, \tag{12}$$

where $T_u\mathcal{U}$ denotes the tangent cone of $\mathcal{U}$ at u and corresponds to the set of all velocities in u that maintain the trajectory in $\mathcal{U}$ (see the formal definition in [79, Chapter 6]). In practical terms, this projection operation ensures that the gradient descent flow never leaves the set $\mathcal{U}$. In the special, but common, case in which $\mathcal{U}$ is an hyper-cube (i.e., each component u_i of u is subject to independent bounds), then the projection operator amounts to an coordinate-wise saturation of the flow.

Multiple technical issues need to be taken care of. We review the most important ones hereafter, pointing at some of the latest efforts in those directions (with a preference for those results that have been specialized to the context of control of power distribution networks).

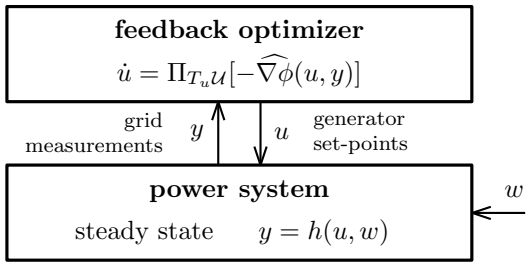

Fig. 8. Feedback implementation of the proposed gradient-descent optimization scheme.

Convergence analysis The vector flow (12) is discontinouous, and the projection operator may be set valued. The existence and uniqueness of solutions of (12), together with its convergence to solutions on (10), depend on opportune regularity assumptions on both ϕ and $\mathcal{U}$. Some of these conditions are derived in [80].

Second-order methods The gradient $\nabla\phi$ can be used to drive iterative optimization schemes that make use of (or estimate) the second derivative of ϕ as well, e.g. quasi-Newton methods. This has been done for example in [81]. Note that once we adopt a descent direction which is not the steepest descent, then the projection on the feasible set $\mathcal{U}$ can become non-trivial, compared to the simpler coordinate-wise saturation that we mentioned before. In second order descent methods, the projection needs to be computed via a nested optimization problem (a quadratic program, in the case of polytopic $\mathcal{U}$). The analysis of convergence when this inner optimization cannot be solved exactly, because of the finite time available, requires special care (see for example [82]).

Time-varying problem parameters The parameters of the optimization problem (10) can vary over time, resulting in some interesting questions on both the existence of solutions to (12) and on its tracking performance with respect to the true minimizer. The case of time-varying exogenous quantities w has been studied for example in [67], [83], while a time-varying feasible region $\mathcal{U}$ has been considered in [84].

E. Feedback Optimization and Robustness

The dynamic flow (12) can be conveniently implemented in a feedback fashion, based on measurements of the output y that are collected from the system (see Figure 8). In fact, we can replace $\nabla\phi(u)$ by

$$\widehat{\nabla\phi}(u,y) := \nabla_u J(u,y) + \nabla_u h(u,w)^\top \nabla_y J(u,y) + \nabla_u h(u,w)^\top \nabla\psi(y) = \nabla\phi(u), \quad (13)$$

where the last equality is valid under the assumption that the output y is at steady state and therefore satisfies the model $y = h(u,w)$.

By adopting $\widehat{\nabla\phi}(u,y)$ as a measurement-based evaluation of the gradient, we drastically reduce the model dependence of the optimization scheme, as $h(u,w)$ does not need to be computed and the only model knowledge that is needed is the *sensitivity matrix* $\nabla_u h(u,w)$. All the remaining terms in $\widehat{\nabla\phi}(u,y)$ are design parameters, and are therefore known.

The sensitivity matrix $\nabla_u h(u,w)$ describes the first-order approximation of the effect of changes in the set-points u on the grid measurements y. A few comments are due.

- In some cases, such as the example presented before, an analytic expression for $\nabla_u h(u,w)$ is available, as a function of both u and w. Namely, $\nabla_u h(u,w)$ can be recovered via the implicit function theorem applied to (8), as both $\nabla_u f(u,y,w)$ and $\nabla_y f(u,y,w)$ are available in analytic form [85]. Under some standard approximations (e.g., DC power flow and $V-\theta$ decoupling) the resulting $\nabla_u h(u,w)$ becomes even independent on u and w.
- Numerical experiments show that approximations of $\nabla_u h(u,w)$ yield very good results when used in the proposed feedback optimization scheme (see for example [83]). A mathematical analysis of the performance of the closed-loop scheme under this source of uncertainty is however still missing.
- As we are assuming that the performance outputs y are measured, the sensitivity matrix $\nabla_u h(u,w)$ can be also inferred from past data, or through *ad-hoc* system identification techniques.

F. Distributed Implementation

According to (13), the real-time computation of a descent direction requires in general a centralized processing of all the performance outputs y and all the set-points u. This reduces scalability of the approach when many microgenerators are connected to the same grid, and a natural question is whether the proposed feedback optimization law can be computed in a distributed manner.

Let us assume with minimal loss of generality that, for each i, the set-point u_i and the measurement y_i are co-located and managed by an agent i. The adoption of separable cost and penalty functions, i.e.

$$J(u,y) = \sum_i J_i(u_i,y_i), \qquad \psi(y) = \sum_i \psi_i(y_i),$$

would partly distribute the computation of each component $\widehat{\nabla\phi}_i(u,y)$ of the gradient. However, from (13), coupling still exists via the matrices $\nabla_u h(u,w)$. As mentioned before, analytic expressions for $\nabla_u h(u,w)$ exist, and these expressions preserve the structure of the system, i.e., they exhibit a sparsity pattern which directly descends from the sparsity of the electrical interconnection between agents. Depending on the choice of set-points and of performance measurements, this sparsity can appear directly in the term $\nabla_u h(u,w)$.

In general, however, we can aim at constructing a sparse matrix Q such that $S := Q\nabla_u h(u,w)^\top$ is also sparse (or even the identity matrix). If Q is positive definite, then the direction $Q\widehat{\nabla\phi}(u,y)$ can be used in the feedback optimization scheme, instead of $\widehat{\nabla\phi}(u,y)$. The resulting direction will still be a descent direction, but not the steepest one. While in general this may affect performance, it is also possible

that the matrix Q can be chosen to approximate the Hessian of the cost function $\phi(u)$, therefore yielding a second order descent flow. This is what happens, for example, in [86]. Note that, as discussed before, special care (and, most likely, extra communication between the agents) will have to be used to compute the projection on the feasible set $\mathcal{U}$.

G. Further extensions

We focused on the gradient descent flow to drive the system to the solution of the optimization problem (9) (or, more precisely, of the optimization problem in which (9b) is replaced by a penalty function). This is clearly not the only solution. We refer the reader to [83], [87], [88] for an alternative approach, in which the inequality constraints of the problem have been dualized, and a saddle-point flow (on an augmented Lagrangian) has been employed to drive the system to a solution of the corresponding KKT equations. Alternatively, in [89] the real-time specifications are expressed using the formalism of semidefinite programming and a dual ϵ subgradient method is proposed. The spirit of these approaches remain the same as in the problem formulation that we presented: to design an output feedback law (i.e., without full state/disturbance measurements) that ensure ultimate convergence to set of minimizer of a given optimization program, while guaranteed satisfaction of a subset of *hard* constraints at all times. Any advance towards the solution of this challenge has the potential to translate immediately into effective solutions for the core goal that we reviewed in this section, which is the autonomous generation of feasible and efficient microgenerator set-points.

IV. Optimal and Distributed Frequency Control of Transmission Grids

A. Frequency Control Background and Fundamentals

All AC power systems are designed to operate only in a very narrow range ($\leq 1\%$) around a nominal frequency value ω_{ref}. The importance of frequency as *the* key control variable in large-scale power systems arises from the physics of SGs. As mentioned in Section II, SGs equipped with standard control systems and interconnected into a large power system will synchronize with one another, converging to a *common* network-wide frequency in steady-state. The difference between this common frequency and the nominal frequency ω_{ref} is directly proportional to the imbalance between demand and scheduled generation in the system. For instance, if demand exceeds scheduled generation, the frequency will settle to a value below ω_{ref}, as illustrated in Figure 4. This relationship forms the basis for the real-time control of supply-demand balance in the system.

Frequency control is performed in power systems on a hierarchy of time-scales [30, Chapter 11.1], ranging from approximately one second to tens of minutes [28, Chapter 9], as shown in Figure 5. Figure 9 shows the response of a typical power system to a sudden and persistent load step (or equivalently, a loss of generation).

From (1), the initial slope of the frequency decrease — the so-called rate-of-change-of-frequency (RoCoF) — is inversely proportional to the inertia of the system; a larger inertia yields a shallower slope. Within a few seconds, speed governors interfaced with SGs through their turbines become active, and SGs inject additional power proportional to the frequency deviation; this slows and eventually stops the drop in frequency. This so-called *primary droop control* mechanism is entirely decentralized.

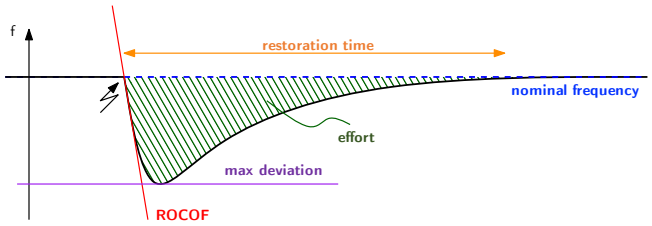

Fig. 9. Response of power system with primary and secondary frequency control to an increase in load; figure adapted from [18].

Primary droop control through the governor system results in a non-zero frequency deviation; the *secondary control* layer restores the frequency to its nominal value on a time-scale of a few minutes. The industry-standard secondary control methodology in interconnected bulk power systems is a semi-decentralized control system called *automatic generation control* (AGC). Finally, on a time-scale of roughly 15 minutes, the nominal generation setpoints of SGs are re-computed via a centralized constrained optimal dispatch; this *tertiary control* layer sits atop the temporal and architectural control hierarchy.

To summarize, in control-theoretic terms, primary frequency control is concerned with *disturbance attenuation* via decentralized proportional control, secondary frequency control is a problem of *asymptotic disturbance rejection* via integral control, and tertiary control deals with *setpoint design*, implemented via centralized feedforward control.

B. The Need for Modernized Frequency Control

For the reasons discussed in Section II, low-inertia power systems are more susceptible to frequency deviations and experience more severe disturbances than classical SG-based systems. Moreover, the standard AGC architecture for secondary control was devised in the 1950's, and has not been substantially updated since then to utilize improvements in communication and computation technologies. With this context, recent research on advanced secondary frequency control has broadly focused on the following questions:

(i) to what extent should the primary/secondary/tertiary control layers be co-designed, and under what circumstances can (or should) they be merged into a single, fast time-scale control architecture?

(ii) what are the appropriate control architectures for integrating large numbers of low-capacity heterogeneous control resources into secondary frequency control, and how should feedback signals be designed to achieve economic objectives and while maintaining (or improving) dynamic performance?

(iii) how can power converter-interfaced resources be most effectively controlled and utilized for frequency control?

A full exploration of these issues is far beyond our scope here; our goal is to introduce the reader to the secondary frequency control problem, identify some of its key characteristics, and note some recent developments.

C. Models for Frequency Control and Key Insights

As secondary frequency control is concerned with asymptotically correcting small deviations in frequency around the nominal value, small-signal models are most appropriate, with reactive power and voltage magnitude dynamics typically neglected. As a representative model for discussion, we consider a network-reduced linearized model of n SGs

$$\Delta\dot{\theta}_i = \Delta\omega_i\,, \tag{14a}$$

$$M_i\Delta\dot{\omega}_i = -D_i\Delta\omega_i + \Delta\tau_{\mathrm{m},i} + \Delta P_{\mathrm{u},i} - \Delta P_{\mathrm{e},i} \tag{14b}$$

$$\Delta P_{\mathrm{e},i} = \sum\nolimits_{j=1}^{n} T_{ij}(\Delta\theta_i - \Delta\theta_j) \tag{14c}$$

$$T_{\mathrm{ch},i}\Delta\dot{\tau}_{\mathrm{m},i} = -\Delta\tau_{\mathrm{m},i} + \Delta\tau_{\mathrm{g},i} \tag{14d}$$

$$T_{\mathrm{g},i}\Delta\dot{\tau}_{\mathrm{g},i} = -\Delta\tau_{\mathrm{g},i} + \Delta u_{\mathrm{m},i} - R_{\mathrm{d},i}^{-1}\Delta\omega_i\,. \tag{14e}$$

The point of linearization for the vectorized state $x = (\theta, \omega, \tau_{\mathrm{m}}, \tau_{\mathrm{g}})$ and vectorized inputs $u = (P_{\mathrm{u}}, u_{\mathrm{m}})$ is

$$x^\star = (\theta^\star, \omega_{\mathrm{ref}}\mathbb{1}_n, \tau_{\mathrm{m}}^\star, \tau_{\mathrm{m}}^\star)\,, \quad u^\star = (P_{\mathrm{u}}^\star, \tau_{\mathrm{m}}^\star)\,,$$

where $\mathbb{1}_n := (1, 1, \ldots, 1)^\top \in \mathbb{R}^n$. Equations (14a)–(14c) describe the linearized mechanical dynamics of a network of SGs; $\Delta P_{\mathrm{u},i} \in \mathbb{R}$ is the uncontrolled injection (generation minus demand) at the same bus as the ith SG, and $\Delta P_{\mathrm{e},i}$ is the electrical power injected by SG i, and $T_{ij} > 0$ is the "synchronizing torque coefficient" for line (i, j) [30, Eq. (11.10)].

The equation (14d) models a non-reheat steam turbine and (14e) models the governor, where $T_{\mathrm{ch},i} > 0$ ($T_{\mathrm{g},i} > 0$) is the turbine (governor) time constant, $R_{\mathrm{d},i} > 0$ is the droop slope (control gain) for primary control, and $\Delta u_{\mathrm{m},i}$ is the external reference for secondary control (the "load reference" setpoint). The reference values $u_{\mathrm{m},i}$ are therefore *set points* to lower-level controllers (Section II-C). The equations (14a)–(14b) also describe reduced-order models of power converters [24]. In any case, the conclusions and development that follow are insensitive to these modeling assumptions, and extend to complex scenarios involving nonlinear models, CIG, load-side participation, and so forth.

To begin our analysis, we consider (14a)–(14e) as together defining a vectorized input-output LTI system

$$\Delta\omega(s) = G_1(s)\Delta P_{\mathrm{u}}(s) + G_2(s)\Delta u_{\mathrm{m}}(s)\,,$$

and examine the response if the disturbances and power references are *constant*. Analysis shows that the open-loop system is input-output stable, and that the DC gain matrices satisfy

$$G_1(0) = G_2(0) := G_0 = \beta^{-1}\mathbb{1}_n\mathbb{1}_n^\top\,. \tag{15}$$

The constant $\beta := \sum_{i=1}^n \beta_i = \sum_{i=1}^n (D_i + R_i^{-1})$ is called the stiffness constant of the power system [30, Eq. (11.9)]. Two immediate control conclusions can be drawn from (15) by applying results from multivariable servoregulator theory [90]. Firstly, since $\operatorname{range} G_0 = \operatorname{span}(\mathbb{1}_n)$, the only admissible steady-state frequency vectors are those with equal entries (i.e., a common steady-state frequency). Moreover, since $\ker G_0 = \{y \in \mathbb{R}^n \mid \sum_{i=1}^n y_i = 0\}$, only the *total sum* of all power references and all uncontrolled disturbances contribute to the common steady-state frequency value. For constant exogenous inputs Δu_{m} and ΔP_{u}, the resulting steady-state frequency deviation $\Delta\omega_{\mathrm{ss}}$ is

$$\Delta\omega_{\mathrm{ss}} = \beta^{-1}\mathbb{1}_n^\top\Delta P_{\mathrm{u}} + \beta^{-1}\mathbb{1}_n^\top\Delta u_{\mathrm{m}}\,. \tag{16}$$

Since G_0 has row rank equal to one, a second conclusion which can be drawn is the following: it is *necessary* that there be *only one frequency integrator* in any internally stable secondary control system (see Appendix I for a short proof).

We conclude that in steady-state (or, by continuity, on sufficiently long time-scales) *a power system acts much like a single-input single-output control system*, with total power imbalance as input and synchronous frequency as output. We conclude that there is incredible flexibility in how to achieve steady-state frequency regulation, both in terms of how frequency measurements can be spatially collected and used for control purposes, and in terms of how steady-state control actions are allocated among actuators in the system. This flexibility permits centralized, distributed, and semi-decentralized approaches to the frequency control problem.

D. Formulation of Optimal Frequency Control Problem

Given the noted flexibility in terms of how steady-state control actions are allocated to actuators in the system, a steady-state optimization problem can be posed by the system operator to minimize the cost of control provision subject to system-wide balance of power[2] (or, equivalently, subject to frequency regulation)[3]

$$\min_{u_{\mathrm{m}}} \quad \sum\nolimits_{i=1}^{n} J_i(u_{\mathrm{m},i}) \tag{17a}$$

$$\text{subject to} \quad \sum\nolimits_{i=1}^{n} (u_{\mathrm{m},i} + P_{\mathrm{u},i}) = 0 \tag{17b}$$

$$u_{\mathrm{m},i} \in \mathcal{U}_i := [\underline{\tau}_{\mathrm{m},i}, \overline{\tau}_{\mathrm{m},i}] \tag{17c}$$

where $\underline{\tau}_{\mathrm{m},i}$ and $\overline{\tau}_{\mathrm{m},i}$ are upper and lower setpoint limits for unit i (cf. (9)) and $J_i : [\underline{\tau}_{\mathrm{m},i}, \overline{\tau}_{\mathrm{m},i}] \to \mathbb{R}$ is the cost rate function of unit i; we assume J_i is convex and differentiable. The formulation (17) assumes that resistive network losses are negligible (standard for transmission system control) and that the grid is sufficiently far from congested scenarios (standard for frequency control).

Going forward, we will assume that the box constraints (17c) have been incorporated into the objective functions J_i via a differentiable penalty function (see [91] for a related approach). With this assumption, the gradient KKT optimality condition for (17) is

$$\nabla J_i(u_{\mathrm{m},i}) = \lambda\,, \qquad i \in \{1, \ldots, n\}\,, \tag{18}$$

[2]This balancing problem will be further studied explicitly in Section V in the context of competitive markets.

[3]We omit additional equality constraints (tie-line flow schedules) for simplicity; see [28, Sec. 9.5.2] for a discussion of tie line flow control.

where $\lambda \in \mathbb{R}$ is the dual variable associated with the power balance constraint (17b). Equation (18) is the famous *economic dispatch criteria*, which states that at optimality the marginal cost for each generation unit should be equal.

E. Control Architectures and Recent Solutions

The problem (17) cannot be solved in a feedforward centralized fashion, as the disturbances $\Delta P_{\mathrm{u},i}$ are unmeasured, spatially distributed, and time-varying. The control problem is to develop feedback controllers to ensure that in closed-loop, the power system converges to an optimizer of (17); this is a problem of *real-time economic balancing*.

Automatic Generation Control The AGC methodology takes a single frequency deviation measurement $\Delta\omega_{\mathrm{AGC}}$, integrates, and broadcasts the resulting control signal[4]:

$$\begin{aligned} \dot{\eta} &= -K_{\mathrm{I}} \cdot b \cdot \Delta\omega_{\mathrm{AGC}} \\ u_{\mathrm{m},i} &= \tau^{\star}_{\mathrm{m},i} + \alpha_i \eta \end{aligned} \tag{19}$$

where $\tau_{\mathrm{f}} > 0$ is the filter time constant, $K_{\mathrm{I}} > 0$ is the integral gain, and $b > 0$ is the frequency bias constant (typically chosen equal to β). The quantity $\alpha_i \geq 0$ is the *participation factor* of unit i at the operating point, defined as

$$\alpha_i := \frac{[\nabla^2 J_i(\tau^{\star}_{\mathrm{m},i})]^{-1}}{\sum_{k=1}^{n}[\nabla^2 J_k(\tau^{\star}_{\mathrm{m},k})]^{-1}}\,, \qquad \sum\nolimits_{i=1}^{n} \alpha_i = 1\,,$$

assuming J_i is twice differentiable. The AGC scheme is centralized and typically treated with quadratic cost functions [31]. See [92]–[95] for overviews and surveys of AGC, and [96] for a more recent treatment.

Gather-and-Broadcast Control A generalization of the AGC scheme collects frequency measurements from across the system, integrates a weighted average, and broadcasts out the control signals:

$$\dot{\eta} = -K_{\mathrm{I}} \sum\nolimits_{i=1}^{n} \mathsf{c}_i \Delta\omega_i \tag{20a}$$

$$u_{\mathrm{m},i} = (\nabla J_i)^{-1}(\eta)\,, \tag{20b}$$

where $K_{\mathrm{I}} > 0$, $\mathsf{c}_i \geq 0$ and $\sum_i \mathsf{c}_i = 1$. The equation (20b) sets the power references of all units based on a *common variable* $\eta(t)$; this common variable converges asymptotically to the marginal cost of system-wide power imbalance (cf. (17)-(18)). This scheme was proposed in [97], which contains a nonlinear Lyapunov stability analysis under a homogeneity assumption on the cost functions.

Distributed Averaging Integral Control Methods from consensus can be leveraged to distribute the integral control computation and thereby remove the centralized point of computation from the previous two methods. Let $A = A^{\top} = [a_{ij}] \in \mathbb{R}^{n\times n}$ denote the adjacency matrix of a connected weighted graph containing a globally reachable node [98]; this models peer-to-peer communication links between SGs. Each unit is assigned an integral variable η_i which serves as a local estimate of the global marginal cost for power imbalance, and evolves according to

$$k_i\dot{\eta}_i = -\Delta\omega_i - \sum\nolimits_{j=1}^{n} a_{ij}(\eta_i - \eta_j) \tag{21a}$$

$$u_{\mathrm{m},i} = (\nabla J_i)^{-1}(\eta_i) \tag{21b}$$

Asymptotically, the consensus feedback in (21a) ensures that all η_i converge towards the optimal price variable λ while eliminating the local frequency deviations; the control actions (21b) are computed just as in (20b). Finally, we note that despite having distributed integral action, this control scheme is entirely consistent with the statement directly below (16); if $\mathsf{w} \in \mathbb{R}^n$ is the left eigenvector associated with the zero eigenvalue of Laplacian matrix of the communication graph [98, Theorem 7.4], then (21a) implies

$$\tfrac{\mathsf{d}}{\mathsf{d}t}\left(\sum\nolimits_{i=1}^{n} \mathsf{w}_i k_i \eta_i\right) = -\sum\nolimits_{i=1}^{n} \mathsf{w}_i \Delta\omega_i$$

which is the integral mode of the controller; all other modes have a stable low-pass characteristic.

There is now an extensive literature on (21), which was initially proposed independently in [53] and [99]. Stability analyses for nonlinear dynamic models can be found in [100]–[103], with communication network design and delay issues treated in [104], [105], and higher-order dynamic models in [106], [107]; see [108], [109] for further microgrid applications. Tuning and fundamental performance limitations have been examined in [110]–[113]. Stability proofs for distributed controller have been restricted to the case of quadratic cost functions J_i; a more general stability proof, e.g., for strictly convex J_i, remains an open problem.

Primal-Dual Control and Other Methods Another popular frequency control approach which we do not cover in detail here is based on continuous-time *saddle point* or *primal-dual* optimization methods; representative references are [114]–[120]. The key idea is to encode system equilibrium and steady-state specifications in an optimization problem, and then apply (augmented) Lagrangian methods to derive an equilibrium-seeking controller; this results in a peer-to-peer distributed control architecture in the same spirit as (21). Centralized and distributed model-predictive control approaches have been proposed in [121]–[124], which allow for transient constraint satisfaction at the expense of implementation complexity. Price-based control strategies have been proposed in [114], [125]–[127], and an approximate decentralized approach was studied in [128]. Finally, we note that there is an emerging line of theoretical research on steady-state optimizing feedback control which encompasses some (or all) of the control schemes discussed in this section; see [70]–[73] for different formulations.

To conclude, we note that important aspects we have not discussed in this section include (i) market-based provision of frequency control services in deregulated power systems, (ii) heterogeneity of resources within the grid, which can allow for control authority to be spread out both spatially and temporally, (iii) balancing authority-based secondary frequency control, where inter-area tie line flows must be

[4]This is a stylized model of AGC, with considerable variation seen in practical implementations; see [30, Section 11.1.6] for further discussion.

regulated to scheduled setpoints, and (iv) practical implementation aspects including delay tolerance and required sampling rates. While advanced control strategies for improving classical frequency control architectures show much promise, practically relevant strategies must in the end be robust, reliable, and simple.

V. Coordination of Energy Supply and Demand

A. Market Mechanisms for Balancing Supply and Demand

In modern, autonomous power grids, supply- and demand-side management, distributed energy generation and storage are seen as among the main facilitators for the integration of renewable energy sources. These technologies have in fact shown the potential to increase energy efficiency via controllable generation, consumption and storage in local balancing markets [129], [130]. In general, active supply and demand management can be referred as programs implemented by system operators or utility companies to efficiently use the available energy, without installing new generation and transmission infrastructure. These include demand response programs, residential and/or commercial load management programs, e.g. for reducing or shifting consumption [131]. The latter aims at shifting the high-power loads to off-peak hours, to reduce the peak-to-average ratio in energy demand. For example, appropriate *load shifting* is foreseen to become crucial for charging/discharging control in areas with high local penetration of plug-in electric vehicles [132].

For load shifting, and in general for balancing supply and demand in electricity markets efficiently, semi-decentralized or distributed *bidding mechanisms*, paired with aggregative *market clearing*, algorithms have been proposed [133], [134]. Namely, a market coordinator controls an incentive variable based on an aggregative measure of energy supply and demand. The latter is determined as an aggregation of individual bids, e.g. computed via local optimization routines. Such coordination mechanism is traditionally in place in the slowest time scale of power system control, and is referred as *tertiary* control, see Figure 5.

While in general, the optimal balancing problem is a hard problem, namely, a mathematical problem with equilibrium constraints (MPEC) [135], simplified, yet representative, models have been proposed. In this section, we model active supply and demand management via *convex optimization* and *monotone game theory*, and review simple incentive mechanisms coupled with iterative bidding for balancing energy supply and demand in a *competitive* setting.

B. Mathematics of Balanced Energy Supply and Demand

We consider N autonomous nodes, e.g. generators, flexible storage and loads, indexed by $i \in \mathcal{I} := \{1, 2, \dots, N\}$, where each shall decide on its power schedule, $u_i = [u_i(1), \dots, u_i(n)]^\top$, over a multi-period horizon of n time periods, from the local decision set $\mathcal{U}_i \subseteq \mathbb{R}^n$, which represents local operational constraints, such as limits, $\underline{u}_i \leq u_i(t) \leq \overline{u}_i$, rate constraints, $|u_i(t+1) - u_i(t)| \leq \delta_i$, and inter-temporal constraints, e.g. $\underline{\sigma}_i \leq \sum_{t=1}^{n} u_i(t) \leq \overline{\sigma}_i$. At each time period $t \in \{1, \dots, n\}$, $u_i(t)$ represents the tertiary control, i.e., the reference input of node i for the secondary control (and $\boldsymbol{u}(t) := [u_1(t), \dots, u_N(t)]^\top$ the vectorized input), as in model (14), Section IV-C. For balancing energy supply ($u_i(t) \geq 0$) and demand ($u_i(t) < 0$) at all times, the power schedules shall be chosen such that

$$\textstyle\sum_{i \in \mathcal{I}} u_i = (\mathbb{1}_N^\top \otimes I_n)\boldsymbol{u} = \mathbb{0}_n \,, \tag{22}$$

where $\boldsymbol{u} := \operatorname{col}(u_1, \dots, u_N)$. Thus, we can define the local feasible set as $\boldsymbol{\mathcal{U}} := \mathcal{U}_1 \times \ldots \times \mathcal{U}_N$, and the coupling constraint set as $\boldsymbol{\mathcal{C}} := \{\boldsymbol{u} \in \mathbb{R}^{nN} \mid (\mathbb{1}_N^\top \otimes I_n)\boldsymbol{u} = \mathbb{0}_n\}$, so that the overall feasible set reads as $\boldsymbol{\mathcal{K}} := \boldsymbol{\mathcal{U}} \cap \boldsymbol{\mathcal{C}}$. Let us assume that all the sets are nonempty, compact and convex and that the set $\boldsymbol{\mathcal{K}}$ satisfies Slater's constraint qualification [136, §5.2.3, (5.26)].

Cooperative balancing If the autonomous nodes belong to the same energy company or agree to *cooperatively* balance energy supply and demand, as in Section IV-D, we can assume that the nodes aim at solving an *economic balancing* optimization problem (17):

$$\begin{cases} \min\limits_{\boldsymbol{u} \in \mathbb{R}^{nN}} & \sum_{i \in \mathcal{I}} J_i(u_i) \\ \text{s.t.} & u_i \in \mathcal{U}_i, \, \forall i \in \mathcal{I} \\ & \sum_{i \in \mathcal{I}} u_i = \mathbb{0}_n. \end{cases} \tag{23}$$

Problem (23) has separable cost function and separable constraints. It is also known as *optimal exchange* problem and, under suitable technical assumptions, be solved efficiently via dual decomposition, Douglas–Rachford (ADMM) and proximal algorithms [137, §7.3.2], [138, §5.3.1]. From an economics perspective, these methods rely on a price adjustment process, so-called *tatonnement*, see the theory of general (Walras) equilibrium [139], [140], [141]. Namely, the market coordinator acts via price adjustments, by increasing or decreasing the price of electricity depending on whether there is an excess demand or excess supply, respectively.

Competitive balancing More realistically, whenever the autonomous nodes belong to different energy parties or companies, it is natural to assume that each node aims at minimizing its local cost function $J_i(u_i, \boldsymbol{u}_{-i})$, which usually depends on both the local variable u_i (first argument), due to the local energy generation or storage cost, and also on the decision variables of the other agents, $\boldsymbol{u}_{-i} = \operatorname{col}((u_j)_{j \neq i})$ (second argument). This is because the electricity price set by the market is typically an aggregative function of all intended power schedules, $u_1, u_2, \dots, u_N$. Formally, we obtain the following *game*, which is a collection of inter-dependent optimization problems:[5]

$$\forall i \in \mathcal{I} : \begin{cases} \min\limits_{u_i \in \mathbb{R}^n} & \sum_{i \in \mathcal{I}} J_i(u_i, \boldsymbol{u}_{-i}) \\ \text{s.t.} & u_i \in \mathcal{U}_i \\ & u_i + \sum_{j \in \mathcal{I} \setminus \{i\}} u_j = \mathbb{0}_n. \end{cases} \tag{24}$$

[5]For each $i \in \mathcal{I}$, with $u_i + \sum_{j \in \mathcal{I} \setminus \{i\}} u_j = \mathbb{0}_n$, we differentiate between the local decision variable, the power schedule u_i, and the given decision variables of the other nodes, the power schedules u_j's.

We note that for each node $i \in \mathcal{I}$, both the cost function J_i and the feasible set,

$$\mathcal{K}_i(\boldsymbol{u}_{-i}) := \left\{ u_i \in \mathcal{U}_i \mid u_i + \textstyle\sum_{j \in \mathcal{I} \setminus \{i\}} u_j = \mathbb{0}_n \right\}, \quad (25)$$

depend on the power schedules of the other nodes, $\boldsymbol{u}_{-i}$.

In this setting, the nodes would *competitively* bid tentative power schedules for ultimately balancing energy supply and demand. In *game theory*, the balancing problem can be seen as that of computing a generalized Nash equilibrium (GNE) of the game in (24) [142], i.e., a set of power schedules $\boldsymbol{u}^* = \mathrm{col}(u_1^*, \dots, u_N^*) \in \boldsymbol{\mathcal{K}}$ such that, for all $i \in \mathcal{I}$,

$$u_i^* \in \operatorname{argmin} \left\{ J_i(v,\, \boldsymbol{u}_{-i}^*) \mid v \in \mathcal{K}_i(\boldsymbol{u}_{-i}^*) \right\}. \quad (26)$$

In plain words, a GNE is such that no node can improve its revenue by unilaterally changing its power schedule to another feasible one. To ensure existence and uniqueness of a v-GNE [143, Prop. 12.7, 12.9], let us assume that the cost functions J_i are continuously differentiable, convex in their first argument, and that the so-called **game mapping**

$$F(\boldsymbol{u}) := \mathrm{col}\left(\nabla_{u_1} J_1(\boldsymbol{u}), \dots, \nabla_{u_N} J_N(\boldsymbol{u}) \right), \quad (27)$$

which collects the local partial derivatives, is *strongly monotone*, i.e., $(F(\boldsymbol{u}) - F(\boldsymbol{v}))^\top (\boldsymbol{u} - \boldsymbol{v}) \geq \varepsilon \|\boldsymbol{u} - \boldsymbol{v}\|$, for some $\varepsilon > 0$, for all $\boldsymbol{u}, \boldsymbol{v}$, and Lipschitz continuous.

C. Operator Theoretic Characterization

In this section, we show the main steps to recast the problem to compute a GNE $\boldsymbol{u}^*$ (26) into a monotone inclusion problem, i.e., the problem to find a *zero* of a monotone operator. First, in order to *decouple* the balance constraint (22) present in (24), we introduce the KKT conditions of each optimization problem in (24). For each node $i \in \mathcal{I}$, let us define its Lagrangian function,

$$L_i(\boldsymbol{u}, \mu_i) := J_i(u_i, \boldsymbol{u}_{-i}) + \iota_{\mathcal{U}_i}(u_i) + \mu_i^\top (\mathbb{1}_N^\top \otimes I_n) \boldsymbol{u}, \quad (28)$$

where $\iota_{\mathcal{U}_i}$ denotes the indicator function[6] and $\mu \in \mathbb{R}^n$ is the *dual multiplier* associated with the balance constraint in (22). Thanks to convexity and regularity, it follows from [143, §12.2.3] that $\boldsymbol{u}^*$ is a GNE of the game in (24) if and only if the following coupled KKT systems hold true:

$$\forall i \in \mathcal{I}: \begin{cases} 0 \;\in\; \nabla_{u_i} J_i(u_i^*, \boldsymbol{u}_{-i}^*) + \mathcal{N}_{\mathcal{U}_i}(u_i^*) + \mu_i \\ 0 \;=\; (\mathbb{1}_N^\top \otimes I_n) \boldsymbol{u}^*, \end{cases} \quad (29)$$

where $\mathcal{N}_{\mathcal{U}_i} = \partial \iota_{\mathcal{U}_i}$ denotes the *normal cone* operator [144, Def. 6.38]. Following the lines in [145], [142, §3.2], for computational convenience, let us look for a *variational* GNE (v-GNE), a solution to the KKT systems in (29) with $\mu_i = \mu \in \mathbb{R}^n$, for all $i \in \mathcal{I}$ [146, §3.2]. Then, to cast the balancing problem in compact form, let us introduce the set-valued mapping

$$T(\boldsymbol{u}, \mu) := \begin{bmatrix} F(\boldsymbol{u}) + \mathcal{N}_{\boldsymbol{\mathcal{U}}}(\boldsymbol{u}) + (\mathbb{1}_N^\top \otimes I_n)^\top \mu \\ -(\mathbb{1}_N^\top \otimes I_n) \boldsymbol{u} \end{bmatrix}, \quad (30)$$

where F is the game mapping in (27) and $\mathcal{N}_{\boldsymbol{\mathcal{U}}} = \mathcal{N}_{\mathcal{U}_1} \times \dots \times \mathcal{N}_{\mathcal{U}_N}$ is the collective normal cone operator. By comparing (29) and (30), we have that $\boldsymbol{u}^*$ is a v-GNE of the competitive balancing game if and only if, for some $\mu^* \in \mathbb{R}^n$, $\mathbb{0} \in T(\boldsymbol{u}^*, \mu^*)$, i.e., $(\boldsymbol{u}^*, \mu^*)$ is a zero of T, which is maximally monotone by construction [144, Def. 20.20]. Therefore, the competitive power balancing problem (24), (26) is a *monotone inclusion* problem [144, §26].

[6] $\iota_{\mathcal{U}_i}(u_i) = 0$ if $u_i \in \mathcal{U}_i$, ∞ otherwise.

D. Coordination Algorithms for Asymptotic Balancing

Monotone inclusion problems, which include convex optimization problems as a special problem class, can be solved efficiently via *operator splitting* methods. In the following subsections, we present two mechanisms for computing a zero of T in (30), i.e., a pair $(\boldsymbol{u}^*, \mu^*)$ such that $\mathbb{0} \in T(\boldsymbol{u}^*, \mu^*)$. In both mechanisms, since the balance constraint is *dualized* (28), energy supply and demand are balanced asymptotically. This is tolerable since balancing mechanisms run off-line to solve the day-ahead market problem, not in real time during the actual power-grid operation.

Dual Decomposition (DD) Algorithm One of the simplest mechanisms to exploit the *dualization* of the balance constraint via the Lagrangian functions in (28) is the so-called *dual decomposition* algorithm:

$$\forall i \in \mathcal{I}: \; u_i(k+1) = \operatorname*{argmin}_{v \in \mathcal{U}_i} J_i(v, \boldsymbol{u}_{-i}(k)) + \mu(k)^\top v \quad (31a)$$

$$\mu(k+1) = \mu(k) + \epsilon \textstyle\sum_{j \in \mathcal{I}} u_j(k+1). \quad (31b)$$

In essence, the DD algorithm consists of a first-order price adjustment mechanism, together with local, full-optimization steps. In (31b), the market coordinator adjusts the pricing variable μ, which, based on the most recent tentative power schedules, is increased if supply exceeds demand, $\sum_j u_j > 0$, and decreased viceversa. We note that if the cost functions, J_i, have an aggregative structure, i.e., $J_i(u_i, \boldsymbol{u}_{-i}) = \tilde{J}_i(u_i, \sum_{j \neq i} u_j)$ for some function $\tilde{J}_i$, which is typical of energy markets, then the algorithm consists of fully decentralized computations, (31a), by the autonomous nodes and of a simple, aggregative computation and broadcast communication, (31b), by the market coordinator. The main advantage of this *optimize-gather-and-broadcast* scheme is that the competing nodes do not need to exchange information among each other.

Under the postulated technical assumptions, for small-enough step size $\epsilon > 0$, the DD algorithm converges to some $(\boldsymbol{u}^*, \mu^*)$ such that $\mathbb{0} \in T(\boldsymbol{u}^*, \mu^*)$, with T as in (30), where $\boldsymbol{u}^*$ is a v-GNE of the balancing game in (24).

Projected Pseudo-Gradient (PPG) Algorithm One practical requirement of the DD algorithm is that at each iteration, each node has to solve an optimization problem (31a). To substantially reduce this computational burden, a viable alternative is to let each node take a single step along the direction of its local pseudo gradient and then project it onto its local constraint set:

$$\forall i \in \mathcal{I}:\ u_i(k+1) = \mathrm{proj}_{\mathcal{U}_i}\left(u_i(k) - \epsilon\left(\nabla_{u_i} J_i(u_i(k), \boldsymbol{u}_{-i}(k)) + \mu(k)\right)\right) \tag{32a}$$

$$\mu(k+1) = \mu(k) + \epsilon \textstyle\sum_{j\in\mathcal{I}} 2u_j(k+1) - u_j(k) \tag{32b}$$

In (32b), we note that the market coordinator performs a second-order price adjustment, while the nodes perform local projected pseudo-gradient steps in (32a). Also for the PPG algorithm, if the cost functions, J_i, have an aggregative structure, then we recover a semi-decentralized computation and communication scheme with the market coordinator in the loop and where the competing nodes shall not exchange information among each other.

The PPG algorithm in (32), also known as *asymmetric projection algorithm* [147, §12.5.1], is the outcome of a preconditioned forward-backward splitting applied to the operator T in (30), splitted as

$$T(\boldsymbol{u}, \mu) = \begin{bmatrix} \mathcal{N}_{\boldsymbol{\mathcal{U}}}(\boldsymbol{u}) + (\mathbb{1}_N^\top \otimes I_n)^\top \mu \\ -(\mathbb{1}_N^\top \otimes I_n)\boldsymbol{u} \end{bmatrix} + \begin{bmatrix} F(\boldsymbol{u}) \\ \mathbb{0}_n \end{bmatrix}. \tag{33}$$

We refer to [148], [149] for the explicit derivation of the algorithm in (32) via operator splitting, for aggregative and network games, respectively. Under the postulated technical assumptions, for small-enough step size $\epsilon > 0$, the algorithm converges to some zero of T in (30), $(\boldsymbol{u}^*, \mu^*)$, where $\boldsymbol{u}^*$ is the unique v-GNE of the game in (24), indeed.

E. Some Recent Semi-Decentralized and Distributed Coordination Algorithms

The literature on coordination algorithms for solving monotone games with general (non-differentiable) convex cost functions and coupling constraints is relatively recent. For the class of aggregative games, such as balancing games, recent contributions span from semi-decentralized incentive mechanisms [150] to distributed coordination [151]. For some classes of network games, distributed algorithms have been recently proposed, e.g. forward-backward with vanishing steps [152] and proximal algorithms [153], [154].

While there is a rich literature on coordination mechanisms that are *generally* applicable to monotone games with balance constraints on energy supply and demand, the class of methods that *best* exploits the problem structure is yet to be identified or perhaps designed.

VI. Conclusions

This tutorial paper has presented an overview of power system control problems stemming from the decrease in inertia occurring in the current power system, including advanced control formulations for power converters, real-time feedback optimization of distribution systems, hierarchical and distributed control methods for transmission system frequency regulation, and decentralized cooperative and competitive algorithms for supply-demand balancing.

Open research challenges pervade all spatial and temporal levels of modern power system control. Aside from specific challenges already emphasized in the previous sections, we highlight the following fruitful avenues for future research.

At the device level, power converters can be efficiently designed as lossless transformers of signals, which means that the impactful control decisions (injecting power) are being taken at the DC terminal. The extent to which the dynamics of converter-interfaced sources can be designed for grid stability appears expansive, with no present consensus on the best strategy. Aggregating many converter-interfaced sources into virtual power plants and controlling the ensemble will also be key for effective integration of renewables.

The flexibility of these devices suggests that their set-point could be regulated in a coordinated way. There seems to be an untapped potential in the real-time control of the steady state of power converters (together with traditional generators) in order to provide faster, fine-grained, and more efficient ancillary services to the grid. Feedback optimization can provide a unified MIMO approach for many real-time control problems that are currently tackled via parallel (and possibly inefficient) SISO controllers.

Finally, at the aggregate system level, merging secondary control and competitive tertiary balancing markets (i.e., market-in-the-loop) is a key direction requiring careful problem formulations and innovative solutions; the extent to which the dynamic response of the system can be decoupled from (or co-designed with) market mechanisms is a crucial question for the viability of such architectures.

Acknowledgements

The authors want to thank their research groups, collaborators, as well as the anonymous reviewers for many fruitful discussions and comments which improved this paper.

References

[1] B. D. Kroposki, "Basic research needs for autonomous energy grids: Summary report of the workshop on autonomous energy grids," National Renewable Energy Laboratory (NREL), Golden, CO (United States), Tech. Rep., September 2017.

[2] T. Ishizaki, A. Chakrabortty, and J.-I. Imura, "Graph-theoretic analysis of power systems," *Proceedings of the IEEE*, vol. 106, no. 5, pp. 931–952, 2018.

[3] A. Chakrabortty and P. P. Khargonekar, "Introduction to wide-area control of power systems." in *ACC*. Citeseer, 2013, pp. 6758–6770.

[4] D. Molzahn, F. Dörfler, H. Sandberg, S. H. Low, S. Chakrabarti, R. Baldick, and J. Lavaei, "A survey of distributed optimization and control algorithms for electric power systems," *IEEE Transactions on Smart Grid*, February 2017, in press.

[5] A. Kargarian, J. Mohammadi, J. Guo, S. Chakrabarti, M. Barati, G. Hug, S. Kar, and R. Baldick, "Toward distributed/decentralized dc optimal power flow implementation in future electric power systems," *IEEE Transactions on Smart Grid*, vol. 9, no. 4, pp. 2574–2594, 2018.

[6] S. H. Low, "Convex relaxation of optimal power flow – part i: Formulations and equivalence," *IEEE Transactions on Control of Network Systems*, vol. 1, no. 1, pp. 15–27, 2014.

[7] ——, "Convex relaxation of optimal power flow – part ii: Exactness," *IEEE Transactions on Control of Network Systems*, vol. 1, no. 2, pp. 177–189, 2014.

[8] J. Beerten, O. Gomis-Bellmunt, X. Guillaud, J. Rimez, A. van der Meer, and D. Van Hertem, "Modeling and control of hvdc grids: a key challenge for the future power system," in *Power Systems Computation Conference (PSCC)*. IEEE, 2014, pp. 1–21.

[9] M. Andreasson, D. V. Dimarogonas, H. Sandberg, and K. H. Johansson, "Distributed controllers for multiterminal hvdc transmission systems," *IEEE Transactions on Control of Network Systems*, vol. 4, no. 3, pp. 564–574, 2017.

[10] D. Zonetti, R. Ortega, and A. Benchaib, "Modeling and control of hvdc transmission systems from theory to practice and back," *Control Engineering Practice*, vol. 45, pp. 133–146, 2015.

[11] L. Meng, Q. Shafiee, G. F. Trecate, H. Karimi, D. Fulwani, X. Lu, and J. M. Guerrero, "Review on control of dc microgrids and multiple microgrid clusters," *IEEE Journal of Emerging and Selected Topics in Power Electronics*, vol. 5, no. 3, pp. 928–948, 2017.

[12] M. Cucuzzella, S. Trip, C. De Persis, X. Cheng, A. Ferrara, and A. van der Schaft, "A robust consensus algorithm for current sharing and voltage regulation in dc microgrids," *IEEE Transactions on Control Systems Technology*, 2018.

[13] S. Moayedi and A. Davoudi, "Unifying distributed dynamic optimization and control of islanded dc microgrids," *IEEE Transactions on Power Electronics*, vol. 32, no. 3, pp. 2329–2346, 2017.

[14] A. Bidram and A. Davoudi, "Hierarchical structure of microgrids control system," *IEEE Transactions on Smart Grid*, vol. 3, no. 4, pp. 1963–1976, 2012.

[15] J. M. Guerrero, J. C. Vásquez, J. Matas, L. G. De Vicuña, and M. Castilla, "Hierarchical control of droop-controlled AC and DC microgrids: a general approach toward standardization," *IEEE Transactions on Industrial Electronics*, vol. 58, no. 1, pp. 158–172, 2011.

[16] C. De Persis and N. Monshizadeh, "Bregman storage functions for microgrid control," *IEEE Transactions on Automatic Control*, vol. 63, no. 1, pp. 53–68, 2018.

[17] J. Fang, H. Li, Y. Tang, and F. Blaabjerg, "On the inertia of future more-electronics power systems," *IEEE Journal of Emerging and Selected Topics in Power Electronics*, 2018.

[18] F. Milano, F. Dörfler, G. Hug, D. J. Hill, and G. Verbič, "Foundations and challenges of low-inertia systems," in *2018 Power Systems Computation Conference (PSCC)*. IEEE, 2018, pp. 1–25.

[19] M.-S. Debry, G. Denis, T. Prevost, F. Xavier, and A. Menze, "Maximizing the penetration of inverter-based generation on large transmission systems: the migrate project," in *6th Solar Integration Workshop*, 2017.

[20] P. Tielens and D. Van Hertem, "The relevance of inertia in power systems," *Renewable and Sustainable Energy Reviews*, vol. 55, pp. 999–1009, 2016.

[21] W. Winter, K. Elkington, G. Bareux, and J. Kostevc, "Pushing the limits: Europe's new grid: Innovative tools to combat transmission bottlenecks and reduced inertia," *IEEE Power and Energy Magazine*, vol. 13, no. 1, pp. 60–74, 2015.

[22] B. Kroposki, B. Johnson, Y. Zhang, V. Gevorgian, P. Denholm, B.-M. Hodge, and B. Hannegan, "Achieving a 100% renewable grid: Operating electric power systems with extremely high levels of variable renewable energy," *IEEE Power and Energy Magazine*, vol. 15, no. 2, pp. 61–73, 2017.

[23] J. A. Taylor, S. V. Dhople, and D. S. Callaway, "Power systems without fuel," *Renewable and Sustainable Energy Reviews*, vol. 57, pp. 1322–1336, 2016.

[24] J. Schiffer, D. Zonetti, R. Ortega, A. M. Stanković, T. Sezi, and J. Raisch, "A survey on modeling of microgrids - from fundamental physics to phasors and voltage sources," *Automatica*, vol. 74, pp. 135–150, 2016.

[25] F. Dörfler, J. W. Simpson-Porco, and F. Bullo, "Electrical networks and algebraic graph theory: Models, properties, and applications," *Proceedings of the IEEE*, vol. 106, no. 5, pp. 977–1005, 2018.

[26] A. van der Schaft and T. Stegink, "Perspectives in modeling for control of power networks," *Annual Reviews in Control*, vol. 41, pp. 119–132, 2016.

[27] O. Ajala, A. D. Domínguez-García, and P. W. Sauer, "A hierarchy of models for inverter-based microgrids," Coordinated Science Laboratory, University of Illinois at Urbana-Champaign, Tech. Rep., 2017.

[28] J. Machowski, J. W. Bialek, and J. R. Bumby, *Power System Dynamics*, 2nd ed. John Wiley & Sons, 2008.

[29] P. W. Sauer and M. A. Pai, *Power System Dynamics and Stability*. Prentice Hall, 1998.

[30] P. Kundur, *Power System Stability and Control*. McGraw-Hill, 1994.

[31] A. J. Wood and B. F. Wollenberg, *Power generation, operation, and control*. John Wiley & Sons, 2012.

[32] Q.-C. Zhong and T. Hornik, *Control of power inverters in renewable energy and smart grid integration*. John Wiley & Sons, 2012, vol. 97.

[33] R. Teodorescu, M. Liserre, and P. Rodriguez, *Grid converters for photovoltaic and wind power systems*. John Wiley & Sons, 2011, vol. 29.

[34] C. Arghir, T. Jouini, and F. Dörfler, "Grid-forming control for power converters based on matching of synchronous machines," *Automatica*, vol. 95, pp. 273–282, September 2018.

[35] S. Y. Caliskan and P. Tabuada, "Compositional transient stability analysis of multimachine power networks," *IEEE Transactions on Control of Network systems*, vol. 1, no. 1, pp. 4–14, 2014.

[36] R. Ortega, A. J. V. D. Schaft, I. Mareels, and B. Maschke, "Putting energy back in control," *IEEE Control Systems Magazine*, vol. 21, no. 2, pp. 18–33, April 2001.

[37] L. Huang, H. Xin, Z. Wang, K. Wu, H. Wang, J. Hu, and C. Lu, "A virtual synchronous control for voltage-source converters utilizing dynamics of dc-link capacitor to realize self-synchronization," *IEEE Journal of Emerging and Selected Topics in Power Electronics*, vol. 5, no. 4, pp. 1565–1577, Dec 2017.

[38] S. Curi, D. Groß, and F. Dörfler, "Control of low-inertia power grids: A model reduction approach," in *Proceedings of the 56th IEEE Conference on Decision and Control*, December 2017, to appear.

[39] I. Cvetkovic, D. Boroyevich, R. Burgos, Y.-H. Hsieh, F. C. Lee, C. Li, and P. Mattavelli, "Experimental verification of a virtual synchronous generator control concept," in *Control and Modeling for Power Electronics (COMPEL), 2016 IEEE 17th Workshop on*. IEEE, 2016, pp. 1–8.

[40] C. Arghir and F. Dörfler, "Direct angle control and energy-shaping techniques for grid-connected converters," *IEEE Transactions on Power Electronics*, March 2019, Submitted. Available at https://www.research-collection.ethz.ch/handle/20.500.11850/331022.

[41] F. Milano, "Power system dynamics visualization for early-stage engineering students and non-technical audience," *EDULEARN 2018, Palma de Mallorca, Spain*, 2018.

[42] D. Groß, C. Arghir, and F. Dörfler, "On the steady-state behavior of a nonlinear power system model," *Automatica*, vol. 90, pp. 248–254, 2018.

[43] D. Groß and F. Dörfler, "On the steady-state behavior of low-inertia power systems," in *IFAC World Congress*, 2017, pp. 10 735–10 741.

[44] C. D. Persis and N. Monshizadeh, "Bregman storage functions for microgrid control," *IEEE Transactions on Automatic Control*, vol. 63, no. 1, pp. 53–68, Jan 2018.

[45] J. W. Simpson-Porco, F. Dörfler, and F. Bullo, "Voltage stabilization in microgrids via quadratic droop control," *IEEE Transactions on Automatic Control*, vol. 62, no. 3, pp. 1239–1253, 2017.

[46] A. J. Wood, B. F. Wollenberg, and G. B. Sheble, *Power Generation, Operation and Control*, 3rd ed. John Wiley and Sons, Inc., 2013.

[47] G. A. van de Wijdeven, A. Jokic, and S. Weiland, "Damping oscillations in electrical power systems: a dissipativity approach," in *Control Applications, 2007. CCA 2007. IEEE International Conference on*. IEEE, 2007, pp. 1079–1084.

[48] R. Ortega, M. Galaz, A. Astolfi, Y. Sun, and T. Shen, "Transient stabilization of multimachine power systems with nontrivial transfer conductances," *IEEE Transactions on Automatic Control*, vol. 50, no. 1, pp. 60–75, 2005.

[49] X. Wu, F. Dörfler, and M. R. Jovanović, "Input-output analysis and decentralized optimal control of inter-area oscillations in power systems," *IEEE Transactions on Power Systems*, vol. 31, no. 3, pp. 2434–2444, 2016.

[50] J. C. Willems, "Paradigms and puzzles in the theory of dynamical systems," *IEEE Transactions on automatic control*, vol. 36, no. 3, pp. 259–294, 1991.

[51] M. Castilla, A. Camacho, P. Martí, M. Velasco, and M. M. Ghahderijani, "Impact of clock drifts on communication-free secondary control schemes for inverter-based islanded microgrids," *IEEE Transactions on Industrial Electronics*, vol. 65, no. 6, pp. 4739–4749, 2018.

[52] J. Schiffer, C. A. Hans, T. Kral, R. Ortega, and J. Raisch, "Modeling, analysis, and experimental validation of clock drift effects in low-inertia power systems," *IEEE Transactions on Industrial Electronics*, vol. 64, no. 7, pp. 5942–5951, 2017.

[53] J. W. Simpson-Porco, F. Dörfler, and F. Bullo, "Synchronization and power sharing for droop-controlled inverters in islanded microgrids," *Automatica*, vol. 49, no. 9, pp. 2603–2611, 2013.

[54] J. Schiffer, R. Ortega, A. Astolfi, J. Raisch, and T. Sezi, "Conditions for stability of droop-controlled inverter-based microgrids," *Automatica*, vol. 50, no. 10, pp. 2457–2469, 2014.

[55] P. Vorobev, P.-H. Huang, M. Al Hosani, J. L. Kirtley, and K. Turitsyn, "A framework for development of universal rules for microgrids

stability and control," in *Decision and Control (CDC), 2017 IEEE 56th Annual Conference on*. IEEE, 2017, pp. 5125–5130.

[56] H. Bevrani, T. Ise, and Y. Miura, "Virtual synchronous generators: A survey and new perspectives," *International Journal of Electrical Power & Energy Systems*, vol. 54, pp. 244–254, 2014.

[57] A. Tayyebi, D. Groß, A. A., K. F., and F. Dörfler, "Interactions of grid-forming power converters and synchronous machines – a comparative study," *IEEE Transactions on Power Systems*, 2019, Submitted. Available at https://arxiv.org/abs/1902.10750.

[58] B. Johnson, M. Rodriguez, M. Sinha, and S. Dhople, "Comparison of virtual oscillator and droop control," in *Control and Modeling for Power Electronics (COMPEL), 2017 IEEE 18th Workshop on*. IEEE, 2017, pp. 1–6.

[59] S. D'Arco and J. Suul, "Virtual synchronous machines – classification of implementations and analysis of equivalence to droop controllers for microgrids," in *IEEE PowerTechs*, 2013.

[60] B. B. Johnson, S. V. Dhople, A. O. Hamadeh, and P. T. Krein, "Synchronization of parallel single-phase inverters with virtual oscillator control," *IEEE Transactions on Power Electronics*, vol. 29, no. 11, pp. 6124–6138, 2014.

[61] L. A. Tôrres, J. P. Hespanha, and J. Moehlis, "Synchronization of identical oscillators coupled through a symmetric network with dynamics: A constructive approach with applications to parallel operation of inverters," *IEEE Transactions on Automatic Control*, vol. 60, no. 12, pp. 3226–3241, 2015.

[62] M. Sinha, F. Dörfler, B. B. Johnson, and S. V. Dhople, "Uncovering droop control laws embedded within the nonlinear dynamics of van der pol oscillators," *IEEE Transactions on Control of Network Systems*, vol. 4, no. 2, pp. 347–358, 2017.

[63] M. Colombino, D. Groß, J. Brouillon, and F. Dörfler, "Global phase and magnitude synchronization of coupled oscillators with application to the control of grid-forming power inverters," *IEEE Transactions on Automatic Control*, 2017, Submitted. Available at https://arxiv.org/abs/1710.00694.

[64] D. Groß, M. Colombino, J. Brouillon, and F. Dörfler, "The effect of transmission-line dynamics on grid-forming dispatchable virtual oscillator control," *IEEE Transactions on Control of Network Systems*, 2018, Submitted. Available at https://arxiv.org/abs/1802.08881.

[65] B. K. Poolla, D. Groß, and F. Dörfler, "Placement and implementation of grid-forming and grid-following virtual inertia and fast frequency response," *IEEE Transactions on Power Systems*, July 2018, To appear. Available at https://arxiv.org/abs/1807.01942.

[66] R. Brown, "Impact of smart grid on distribution system design," in *Proc. IEEE Power and Energy Society General Meeting*, 2008.

[67] A. Bernstein, E. Dall'Anese, and A. Simonetto, "Online optimization with feedback," *arXiv:1804.05159*, 2018.

[68] L. S. Lawrence, J. W. Simpson-Porco, and E. Mallada, "The optimal steady-state control problem," *arXiv:1810.12892*, 2018. [Online]. Available: https://arxiv.org/pdf/1810.12892

[69] M. Colombino, E. Dall'Anese, and A. Bernstein, "Online optimization as a feedback controller: Stability and tracking," *arXiv:1805.09877*, 2018. [Online]. Available: https://arxiv.org/pdf/1805.09877

[70] L. S. P. Lawrence, J. W. Simpson-Porco, and E. Mallada, "The optimal steady-state control problem," *IEEE Transactions on Automatic Control*, 2018, submitted.

[71] M. Colombino, E. Dall'Anese, and A. Bernstein, "Online optimization as a feedback controller: stability and tracking," *arXiv:1805.09877[math.OC]*, 2018.

[72] Z. E. Nelson and E. Mallada, "An integral quadratic constraint framework for real-time steady-state optimization of linear time-invariant systems," in *Proc. American Control Conference*, 2018.

[73] S. Menta, A. Hauswirth, S. Bolognani, G. Hug, and F. Dörfler, "Stability of dynamic feedback optimization with applications to power systems," in *Allerton Conf. on Communications, Control and Computing*, Sep. 2018.

[74] S. Bolognani and S. Zampieri, "On the existence and linear approximation of the power flow solution in power distribution networks," *IEEE Transactions on Power Systems*, vol. 31, no. 1, pp. 163–172, Jan. 2016.

[75] A. Bernstein, C. Wang, E. Dall'Anese, J.-Y. Le Boudec, and C. Zhao, "Load flow in multiphase distribution networks: Existence, uniqueness, non-singularity and linear models," *IEEE Transactions on Power Systems*, vol. 33, no. 6, pp. 5832–5843, Nov. 2018.

[76] E. Dall'Anese, H. Zhu, and G. B. Giannakis, "Distributed Optimal Power Flow for Smart Microgrids," *IEEE Trans. Smart Grid*, vol. 4, no. 3, pp. 1464–1475, Sep. 2013.

[77] Q. Peng and S. H. Low, "Distributed optimal power flow algorithm for radial networks, I: Balanced single phase case," *IEEE Transactions on Smart Grid*, vol. 9, no. 1, pp. 111–121, Jan. 2018.

[78] L. Gan and S. H. Low, "An Online Gradient Algorithm for Optimal Power Flow on Radial Networks," *IEEE J. Sel. Areas Commun.*, vol. 34, no. 3, pp. 625–638, Mar. 2016.

[79] R. T. Rockafellar and R. J. Wets, *Variational Analysis*, 3rd ed. Springer, 1998.

[80] A. Hauswirth, S. Bolognani, and F. Dörfler, "Projected dynamical systems on irregular, non-Euclidean domains for nonlinear optimization," *arXiv:1809.04831 [math.OC]*, Sep. 2018.

[81] Y. Tang, K. Dvijotham, and S. Low, "Real-time optimal power flow," *IEEE Transactions on Smart Grid*, vol. 8, no. 6, pp. 2963–2973, 2017.

[82] G. Qu and N. Li, "An optimal and distributed feedback voltage control under limited reactive power," in *Proc. Power Systems Computation Conference (PSCC)*, 2018.

[83] E. Dall'Anese and A. Simonetto, "Optimal Power Flow Pursuit," *IEEE Trans. Smart Grid*, no. 2, pp. 942–952, 2018.

[84] A. Hauswirth, I. Subotic, S. Bolognani, G. Hug, and F. Dörfler, "Time-varying projected dynamical systems with applications to feedback optimization of power systems," in *Proc. 57th IEEE Conference on Decision and Control*, 2018.

[85] S. Bolognani and F. Dörfler, "Fast power system analysis via implicit linearization of the power flow manifold," in *Proc. 53rd Annual Allerton Conference on Communication, Control, and Computing*, 2015.

[86] S. Bolognani, R. Carli, G. Cavraro, and S. Zampieri, "Distributed Reactive Power Feedback Control for Voltage Regulation and Loss Minimization," *IEEE Trans. Automatic Control*, vol. 60, no. 4, pp. 966–981, 2015.

[87] Y. Tang, E. Dall'Anese, A. Bernstein, and S. H. Low, "A feedback-based regularized primal-dual gradient methodfor time-varying nonconvex optimization," in *Proc. IEEE Conf. Decision and Control*, 2018.

[88] A. Bernstein and E. Dall'Anese, "Real-time feedback-based optimization of distribution grids: A unified approach," *arXiv:1711.01627 [math.OC]*, 2017.

[89] E. Dall'Anese, S. V. Dhople, and G. B. Giannakis, "Photovoltaic Inverter Controllers Seeking AC Optimal Power Flow Solutions," *IEEE Transactions on Power Systems*, vol. 31, no. 4, pp. 2809–2823, 2016.

[90] E. Davison, "The robust control of a servomechanism problem for linear time-invariant multivariable systems," *IEEE Transactions on Automatic Control*, vol. 21, no. 1, pp. 25–34, 1976.

[91] A. Cherukuri and J. Cortés, "Initialization-free distributed coordination for economic dispatch under varying loads and generator commitment," *Automatica*, vol. 74, pp. 183 – 193, 2016.

[92] H. Glavitsch and J. Stoffel, "Automatic generation control," *International Journal of Electrical Power & Energy Systems*, vol. 2, no. 1, pp. 21 – 28, 1980.

[93] J. Carpentier, "To be or not to be modern, that is the question for automatic generation control (point of view of a utility engineer)," *International Journal of Electrical Power & Energy Systems*, vol. 7, no. 2, pp. 81 – 91, 1985.

[94] N. Jaleeli, L. S. VanSlyck, D. N. Ewart, L. H. Fink, and A. G. Hoffmann, "Understanding automatic generation control," *IEEE Transactions on Power Systems*, vol. 7, no. 3, pp. 1106–1122, 1992.

[95] P. K. Ibraheem and D. P. Kothari, "Recent philosophies of automatic generation control strategies in power systems," *IEEE Transactions on Power Systems*, vol. 20, no. 1, pp. 346–357, 2005.

[96] D. Apostolopoulou, P. W. Sauer, and A. D. Dominguez-Garcia, "Automatic generation control and its implementation in real time," in *Hawaii International Conference on System Sciences*, Waikoloa, HI, USA, Jan. 2014, pp. 2444–2452.

[97] F. Dörfler and S. Grammatico, "Gather-and-broadcast frequency control in power systems," *Automatica*, vol. 79, pp. 296 – 305, 2017.

[98] F. Bullo, *Lectures on Network Systems*, 1st ed. CreateSpace, 2018, with contributions by J. Cortes, F. Dorfler, and S. Martinez. [Online]. Available: http://motion.me.ucsb.edu/book-lns

[99] M. Andreasson, D. V. Dimarogonas, K. H. Johansson, and H. Sandberg, "Distributed vs. centralized power systems frequency control

under unknown load changes," in *European Control Conference*, Zürich, Switzerland, Jul. 2013, pp. 3524–3529.

[100] C. Zhao, E. Mallada, and F. Dörfler, "Distributed frequency control for stability and economic dispatch in power networks," in *American Control Conference*, Chicago, IL, USA, Jul. 2015, pp. 2359–2364.

[101] F. Dörfler, J. W. Simpson-Porco, and F. Bullo, "Breaking the hierarchy: Distributed control & economic optimality in microgrids," *IEEE Transactions on Control of Network Systems*, vol. 3, no. 3, pp. 241–253, 2016.

[102] S. Trip, M. Bürger, and C. D. Persis, "An internal model approach to (optimal) frequency regulation in power grids with time-varying voltages," *Automatica*, vol. 64, pp. 240 – 253, 2016.

[103] E. Weitenberg, C. D. Persis, and N. Monshizadeh, "Exponential convergence under distributed averaging integral frequency control," *Automatica*, vol. 98, pp. 103 – 113, 2018.

[104] X. Wu, F. Dörfler, and M. R. Jovanović, "Topology identification and design of distributed integral action in power networks," in *American Control Conference*, Jul. 2016, pp. 5921–5926.

[105] J. Schiffer, F. Dörfler, and E. Fridman, "Robustness of distributed averaging control in power systems: Time delays & dynamic communication topology," *Automatica*, vol. 80, pp. 261 – 271, 2017.

[106] S. Trip and C. D. Persis, "Distributed optimal load frequency control with non-passive dynamics," *IEEE Transactions on Control of Network Systems*, vol. PP, no. 99, pp. 1–1, 2017.

[107] A. Kasis, N. Monshizadeh, and I. Lestas, "A novel distributed secondary frequency control scheme for power networks with high order turbine governor dynamics," in *European Control Conference*, Jun. 2018, pp. 2569–2574.

[108] S. T. Cady, A. D. Domínguez-García, and C. N. Hadjicostis, "A distributed generation control architecture for islanded ac microgrids," *IEEE Transactions on Control Systems Technology*, vol. 23, no. 5, pp. 1717–1735, 2015.

[109] J. Llanos, D. E. Olivares, J. W. Simpson-Porco, M. Kazerani, and D. Saez, "A novel distributed control strategy for optimal dispatch of isolated microgrids considering congestion," *IEEE Transactions on Smart Grid*, May 2019, submitted.

[110] E. Tegling, M. Andreasson, J. W. Simpson-Porco, and H. Sandberg, "Improving performance of droop-controlled microgrids through distributed PI-control," in *American Control Conference*, Boston, MA, USA, Jul. 2016, pp. 2321–2327.

[111] E. Tegling and H. Sandberg, "On the coherence of large-scale networks with distributed pi and pd control," *IEEE Control Systems Letters*, vol. 1, no. 1, pp. 170–175, 2017.

[112] M. Andreasson, E. Tegling, H. Sandberg, and K. H. Johansson, "Coherence in synchronizing power networks with distributed integral control," in *IEEE Conf. on Decision and Control*, Melbourne, Australia, Dec. 2017, pp. 6327–6333.

[113] H. Flamme, E. Tegling, and H. Sandberg, "Performance limitations of distributed integral control in power networks under noisy measurements," in *American Control Conference*, Milwaukee, WI, USA, Jun. 2018, pp. 5380–5386.

[114] A. Jokić, M. Lazar, and P. P. J. V. den Bosch, "Real-time control of power systems using nodal prices," *International Journal of Electrical Power & Energy Systems*, vol. 31, no. 9, pp. 522–530, 2009.

[115] N. Li, C. Zhao, and L. Chen, "Connecting automatic generation control and economic dispatch from an optimization view," *IEEE Transactions on Control of Network Systems*, vol. 3, no. 3, pp. 254–264, Sep. 2016.

[116] X. Zhang and A. Papachristodoulou, "A real-time control framework for smart power networks: Design methodology and stability," *Automatica*, vol. 58, pp. 43–50, 2015.

[117] E. Mallada, C. Zhao, and S. Low, "Optimal load-side control for frequency regulation in smart grids," *IEEE Transactions on Automatic Control*, vol. 62, no. 12, pp. 6294–6309, 2017.

[118] C. Zhao, E. Mallada, S. H. Low, and J. Bialek, "Distributed plug-and-play optimal generator and load control for power system frequency regulation," *International Journal of Electrical Power & Energy Systems*, vol. 101, pp. 1 – 12, 2018.

[119] Z. Wang, F. Liu, J. Z. F. Pang, S. Low, and S. Mei, "Distributed optimal frequency control considering a nonlinear network-preserving model," *IEEE Transactions on Power Systems*, pp. 1–1, 2018.

[120] A. Kasis, N. Monshizadeh, E. Devane, and I. Lestas, "Stability and optimality of distributed secondary frequency control schemes in power networks," *IEEE Transactions on Smart Grid*, pp. 1–1, 2018.

[121] A. N. Venkat, I. A. Hiskens, J. B. Rawlings, and S. J. Wright, "Distributed mpc strategies with application to power system automatic generation control," *IEEE Transactions on Control Systems Technology*, vol. 16, no. 6, pp. 1192–1206, 2008.

[122] A. M. Ersdal, L. Imsland, and K. Uhlen, "Model predictive load-frequency control," *IEEE Transactions on Power Systems*, vol. 31, no. 1, pp. 777–785, 2016.

[123] J. Köhler, M. A. Müller, N. Li, and F. Allgöwer, "Real time economic dispatch for power networks: A distributed economic model predictive control approach," in *IEEE Conf. on Decision and Control*, Dec. 2017, pp. 6340–6345.

[124] P. R. B. Monasterios and P. Trodden, "Low-complexity distributed predictive automatic generation control with guaranteed properties," *IEEE Transactions on Smart Grid*, vol. 8, no. 6, pp. 3045–3054, 2017.

[125] T. Stegink, C. D. Persis, and A. van der Schaft, "A unifying energy-based approach to stability of power grids with market dynamics," *IEEE Transactions on Automatic Control*, vol. 62, no. 6, pp. 2612–2622, Jun. 2017.

[126] T. Stegink, A. Cherukuri, C. D. Persis, A. V. D. Schaft, and J. Cortés, "Integrating iterative bidding in electricity markets and frequency regulation," in *American Control Conference*, Jun. 2018, pp. 6182–6187.

[127] T. Stegink, A. Cherukuri, C. D. Persis, A. V. D. Schaft, and J. Cortes, "Stable interconnection of continuous-time price-bidding mechanisms with power network dynamics," Jun. 2018, pp. 1–6.

[128] E. Weitenberg, Y. Jiang, C. Zhao, E. Mallada, C. D. Persis, and F. Dörfler, "Robust decentralized secondary frequency control in power systems: Merits and trade-offs," *IEEE Transactions on Automatic Control*, pp. 1–1, 2018.

[129] A.-H. Mohsenian-Rad, V. Wong, J. Jatskevich, R. Schober, and A. Leon-Garcia, "Autonomous demand-side management based on game-theoretic energy consumption scheduling for the future smart grid," *IEEE Trans. on Smart Grid*, vol. 1, no. 3, pp. 320–331, 2010.

[130] I. Atzeni, L. Ordonez, G. Scutari, D. Palomar, and J. R. Fonollosa, "Demand-side management via distributed energygeneration and storage optimization," *IEEE Trans. on Smart Grid*, vol. 4, no. 2, pp. 866–876, 2013.

[131] C. W. Gellings and J. H. Chamberlin, *Demand Side Management: Concepts and Methods*, P. Books, Ed., 1993.

[132] Z. Ma, D. Callaway, and I. Hiskens, "Decentralized charging control of large populations of plug-in electric vehicles," *IEEE Trans. on Control Systems Technology*, vol. 21, no. 1, pp. 67–78, 2013.

[133] W. David, "Strategic bidding in competitive electricity markets - a literature survey," in *Power Engineering Society Summer Meeting*, 2000.

[134] D. L. Torre, Contreras, and Conejo, "Finding multiperiod Nash equilibria in pool-based electricity markets," *IEEE Trans. Power Systems*, vol. 19, no. 1, pp. 643–651, 2004.

[135] B. Hobbs, C. Metzler, and J. Pang, "Strategic gaming analysis for electric power systems: An MPEC approach," *IEEE Transactions on Power Systems*, vol. 15, no. 2, pp. 638–645, 2000.

[136] S. Boyd and L. Vandenberghe, *Convex Optimization*. Cambridge University Press, 2009.

[137] S. Boyd, N. Parikh, E. Chu, B. Peleato, and J. Eckstein, "Distributed optimization and statistical learning via the alternating direction method of multipliers," *Foundations and Trends® in Machine Learning*, vol. 3, no. 1, pp. 1–122, 2011.

[138] N. Parikh and S. Boyd, "Proximal algorithms," *Foundations and Trends in Optimization*, vol. 1, no. 3, pp. 123—-231, 2013.

[139] K. Arrow and G. Debreu, "Existence of an equilibrium for a competitive economy," *Econometrica*, vol. 22, no. 3, pp. 265–290, 1954.

[140] H. Uzawa, "Market mechanisms and mathematical programming," *Econometrica*, vol. 28, no. 4, pp. 872–881, 1960.

[141] ——, "Walras' tatonnement in the theory of exchange," *The Review of Economic Studies*, vol. 27, no. 3, pp. 182—194, 1960.

[142] F. Facchinei and C. Kanzow, "Generalized Nash equilibrium problems," *A Quarterly Journal of Operations Research, Springer*, vol. 5, pp. 173–210, 2007.

[143] D. Palomar and Y. Eldar, *Convex optimization in signal processing and communication*. Cambridge University Press, 2010.

[144] H. H. Bauschke, P. L. Combettes *et al.*, *Convex analysis and monotone operator theory in Hilbert spaces*, 2nd ed. Springer, 2017.

[145] A. A. Kulkarni and U. Shanbhag, "On the variational equilibrium as a refinement of the generalized Nash equilibrium," *Automatica*, vol. 48, pp. 45–55, 2012.
[146] A. Auslender and M. Teboulle, "Lagrangian duality and related multiplier methods for variational inequality problems," *SIAM Journal on Optimization*, vol. 10, no. 4, pp. 1097–1115, 2000.
[147] F. Facchinei and J.-S. Pang, *Finite-dimensional variational inequalities and complementarity problems*. Springer Science & Business Media, 2007.
[148] G. Belgioioso and S. Grammatico, "Projected-gradient algorithms for generalized equilibrium seeking in aggregative games are preconditioned forward-backward methods," in *Proc. of the IEEE European Control Conference*, 2018.
[149] P. Yi and L. Pavel, "An operator splitting approach for distributed generalized nash equilibria computation," *Automatica*, vol. 102, pp. 111–121, 2019.
[150] S. Grammatico, "Dynamic control of agents playing aggregative games with coupling constraints," *IEEE Trans. on Automatic Control*, vol. 62, no. 9, pp. 4537 – 4548, 2017.
[151] J. Koshal, A. Nedić, and U. Shanbhag, "Distributed algorithms for aggregative games on graphs," *Operations Research*, vol. 64, no. 3, pp. 680–704, 2016.
[152] A. Kannan and U. V. Shanbhag, "Distributed computation of equilibria in monotone nash games via iterative regularization techniques," *SIAM Journal on Optimization*, vol. 22, no. 4, pp. 1177–1205, 2012.
[153] P. Yi and L. Pavel, "Distributed generalized Nash equilibria computation of monotone games via double-layer preconditioned proximal-point algorithms," *IEEE Transactions on Control of Network Systems*, 2018.
[154] G. Belgioioso and S. Grammatico, "A distributed proximal-point algorithm for Nash equilibrium seeking in generalized potential games with linearly coupled costs," in *Proc. of the European Control Conference*, 2019.

APPENDIX I
INTEGRAL CONTROL AND THE DC GAIN

Consider the linear time-invariant system

$$\begin{aligned} \dot{x} &= Ax + Bu + Pw \\ e &= Cx + Qw \end{aligned} \tag{34}$$

with state $x \in \mathbb{R}^n$, control input $u \in \mathbb{R}^m$, constant exogenous signal $w \in \mathbb{R}^{n_w}$, and tracking error output $e \in \mathbb{R}^p$ where $p \leq m$. Assume that A is Hurwitz, and let $G(s) := C(sI_n - A)^{-1}B$ denote the transfer matrix from u to e. Suppose we wish to perform integral control on some number $r \leq p$ of the error outputs e. Let $F \in \mathbb{R}^{r \times p}$ with $\operatorname{rank} F = r$ be the matrix which selects the desired outputs, and set

$$\dot{\eta} = Fe \tag{35}$$

as the required integral variables. The PBH test implies that the interconnection of (34) and (35) is stabilizable using the control u if and only if the block matrix

$$\left[\begin{array}{cc|c} A & \mathbb{0} & B \\ FC & \mathbb{0} & \mathbb{0} \end{array}\right]$$

has full row rank. Elementary row and column operations quickly show that this rank condition holds if and only if $\operatorname{rank} FG(0) = r$. Suppose now that $\operatorname{rank} G(0) < r$. Then

$$\operatorname{rank} FG(0) \leq \min\{\operatorname{rank} F, \operatorname{rank} G(0)\} < r$$

shows that the cascade is not stabilizable. It is thus necessary for stabilizability that $\operatorname{rank} G(0) \geq r$, or, put differently, that the number of integrators be no more than $\operatorname{rank} G(0)$.